This is a repository copy of *Measurement of electroweak Z(νν) γjj production and limits on anomalous quartic gauge couplings in pp collisions at s√ = 13 TeV with the ATLAS detector*.

White Rose Research Online URL for this paper:
https://eprints.whiterose.ac.uk/200626/

Version: Published Version

Article:
Aad, G., Abbott, B., Abbott, D.C. et al. (2908 more authors) (2023) Measurement of electroweak Z(νν) γjj production and limits on anomalous quartic gauge couplings in pp collisions at s√ = 13 TeV with the ATLAS detector. Journal of High Energy Physics, 2023. 82.

https://doi.org/10.1007/jhep06(2023)082

Reuse
This article is distributed under the terms of the Creative Commons Attribution (CC BY) licence. This licence allows you to distribute, remix, tweak, and build upon the work, even commercially, as long as you credit the authors for the original work. More information and the full terms of the licence here: https://creativecommons.org/licenses/

Takedown
If you consider content in White Rose Research Online to be in breach of UK law, please notify us by emailing eprints@whiterose.ac.uk including the URL of the record and the reason for the withdrawal request.

eprints@whiterose.ac.uk
https://eprints.whiterose.ac.uk/

Published for SISSA by Springer

Received: August 29, 2022
Revised: November 9, 2022
Accepted: December 4, 2022
Published: June 14, 2023

Measurement of electroweak $Z(\nu\bar{\nu})\gamma jj$ production and limits on anomalous quartic gauge couplings in pp collisions at $\sqrt{s} = 13$ TeV with the ATLAS detector

The ATLAS collaboration

E-mail: atlas.publications@cern.ch

Abstract: The electroweak production of $Z(\nu\bar{\nu})\gamma$ in association with two jets is studied in a regime with a photon of high transverse momentum above 150 GeV using proton–proton collisions at a centre-of-mass energy of 13 TeV at the Large Hadron Collider. The analysis uses a data sample with an integrated luminosity of 139 fb^{-1} collected by the ATLAS detector during the 2015–2018 LHC data-taking period. This process is an important probe of the electroweak symmetry breaking mechanism in the Standard Model and is sensitive to quartic gauge boson couplings via vector-boson scattering. The fiducial $Z(\nu\bar{\nu})\gamma jj$ cross section for electroweak production is measured to be $0.77^{+0.34}_{-0.30}$ fb and is consistent with the Standard Model prediction. Evidence of electroweak $Z(\nu\bar{\nu})\gamma jj$ production is found with an observed significance of 3.2σ for the background-only hypothesis, compared with an expected significance of 3.7σ. The combination of this result with the previously published ATLAS observation of electroweak $Z(\nu\bar{\nu})\gamma jj$ production yields an observed (expected) signal significance of 6.3σ (6.6σ). Limits on anomalous quartic gauge boson couplings are obtained in the framework of effective field theory with dimension-8 operators.

Keywords: Electroweak Interaction, Hadron-Hadron Scattering

ArXiv ePrint: 2208.12741

Open Access, Copyright CERN,
for the benefit of the ATLAS Collaboration.
Article funded by SCOAP^3.

https://doi.org/10.1007/JHEP06(2023)082

JHEP06(2023)082

Contents

1 Introduction **1**

2 Experimental set-up **3**

3 Data and simulation **3**

4 Event reconstruction and selection **5**
4.1 Object reconstruction 5
4.2 Region definitions 6

5 Background estimation **8**

6 Systematic uncertainties **10**

7 Signal extraction procedure and results **12**

8 Combination with previous ATLAS measurement **14**

9 Limits on anomalous quartic gauge couplings **18**

10 Conclusion **21**

The ATLAS collaboration **29**

JHEP06(2023)082

1 Introduction

The scattering of two vector bosons (VBS), $VV \to VV$ with $V = W/Z/\gamma$, is an important process to probe the nature of electroweak (EWK) symmetry breaking in the Standard Model (SM). The presence of the Higgs field in the SM prevents the divergence of VBS amplitudes at high energies and violation of unitarity at the TeV scale. The non-Abelian structure of gauge interactions in the electroweak sector of the Standard Model results in a rich variety of VBS processes, with unique opportunities to probe physics beyond the SM (BSM). VBS processes are sensitive to SM quartic gauge couplings (QGCs) and also to possible anomalous QGCs (aQGCs) [1–3].

Neutral QGCs are absent in the SM at tree level, but they can be induced by BSM physics, allowing new processes at high energy scales. The vector-boson scattering $Z\gamma$ process and a similar process exploiting the ZZ final state are the only processes sensitive to the neutral quartic gauge couplings, with the former having the larger expected cross section. Such processes can be studied through measurements of the electroweak production of two vector bosons and two jets ($VVjj$).

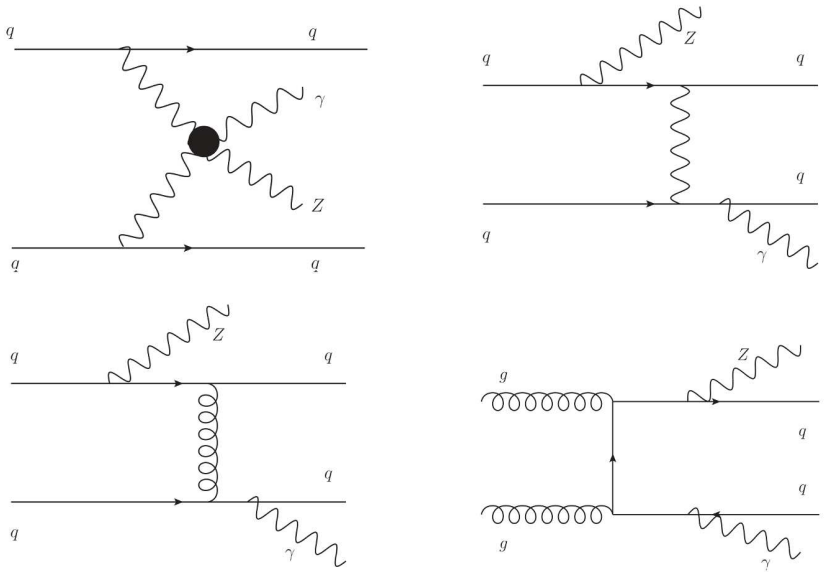

Figure 1. Feynman diagrams of electroweak $Z\gamma jj$ production involving the VBS subprocess (top left) or non-VBS subprocesses (top right) and of QCD $Z\gamma jj$ production with gluon exchange (bottom left) or the s-channel gg–qq process (bottom right).

The $Z\gamma jj$ final states are produced mainly through a combination of strong and electroweak interactions in proton–proton (pp) collisions. The signal in this study is of the order α^4_{EWK} at tree level, where α_{EWK} is the electroweak coupling constant. In the following, such processes are referred to as $Z\gamma jj$ EWK. The VBS process is an inseparable part of the gauge-invariant ensemble of $Z\gamma jj$ electroweak processes [4]. The main background in this study is of order $\alpha^2_{\text{s}}\alpha^2_{\text{EWK}}$ at tree level, where α_{s} is the quantum chromodynamics (QCD) strong coupling constant. In the following, such processes are referred to as $Z\gamma jj$ QCD. Example Feynman diagrams of the aforementioned processes are given in figure 1.

This paper presents a measurement of electroweak production in the $Z\gamma jj$ final state, where the Z boson decays into $\nu\bar{\nu}$. This choice is motivated by the fact that the Z boson branching ratio into neutrinos is larger than the branching ratio into charged leptons; also, the background is under better control than in the hadronic decay channel. The analysis uses pp collision data recorded between 2015 and 2018 by the ATLAS detector [5] during Run 2 at the LHC. Based on this measurement, a search for aQGCs is performed. Anomalous couplings produce deviations from the SM prediction that grow with increasing momentum transfer between the incoming partons. Hence, this analysis exploits a region of high momentum transfer by requiring a photon of transverse momentum larger than 150 GeV.

The high energy and luminosity of the LHC allow rare VBS processes to be studied in detail. In particular, the observation of the $Z(\ell\bar{\ell})\gamma jj$ channel has been reported [6]. Moreover, the observation of $Z(\nu\bar{\nu})\gamma jj$ has been reported [7] in a low-energy phase-space region orthogonal to that presented in this paper. While the low-energy phase space gives negligible sensitivity for the aQGC search, it can be combined with the current high-energy

JHEP06(2023)082

analysis to increase the overall sensitivity to the SM electroweak $Z(\nu\bar{\nu})\gamma jj$ process. Other $VVjj$ EWK processes, including $ZZjj$ [8], $W\gamma jj$ [9], same-sign $WWjj$ [10], $W^{\pm}Zjj$ [11], and photon-induced $W^{+}W^{-}jj$ [12], have also been observed.

2 Experimental set-up

The ATLAS detector [5] is a multi-purpose particle detector with a forward–backward symmetric cylindrical geometry and coverage of nearly the entire solid angle.[1] It consists of an inner tracking detector (ID) surrounded by a thin superconducting solenoid providing a 2 T axial magnetic field, electromagnetic (ECAL) and hadronic (HCAL) calorimeters, and a muon spectrometer (MS).

The ID is used for precise measurements of charged-particle tracks. It is composed of two silicon detectors covering the pseudorapidity range $|\eta| < 2.5$: a pixel detector (including the insertable B-layer [13, 14]) and a silicon microstrip tracker, surrounded by a straw-tube transition radiation tracker (TRT) with an acceptance of $|\eta| < 2.0$, which also contributes to electron identification.

The ECAL is composed of high-granularity lead/liquid-argon (LAr) calorimeters in the region $|\eta| < 3.2$ and copper/LAr calorimeters in the region $3.2 < |\eta| < 4.9$. It plays a crucial role in photon identification, since photons are identified as narrow isolated showers in the ECAL. The HCAL consists of a steel/scintillator-tile calorimeter within $|\eta| < 1.7$ and two copper/LAr and tungsten/LAr forward calorimeters within $1.7 < |\eta| < 4.9$. The fine segmentation of the ATLAS calorimeter system allows efficient separation of jets from isolated prompt photons.

The MS comprises three large superconducting toroids, each having eight coils, as well as trigger and high-precision tracking chamber systems that cover the regions $|\eta| < 2.4$ and $|\eta| < 2.7$, respectively.

The ATLAS trigger system [15] has two levels, a hardware-based first-level trigger and a software-based high-level trigger (HLT). The trigger system selects events from the 40 MHz LHC proton bunch crossings at a rate of about 1 kHz.

An extensive software suite [16] is used in the reconstruction and analysis of real and simulated data, in detector operations, and in the trigger and data acquisition systems of the experiment.

3 Data and simulation

The analysis uses the data collected by the ATLAS experiment from LHC pp collisions at a centre-of-mass energy of $\sqrt{s} = 13$ TeV during 2015–2018 stable beam conditions, when all subdetectors were operational [17], corresponding to a total integrated luminosity of $139\,\text{fb}^{-1}$ [18, 19].

[1] A right-handed coordinate system is used with its origin at the nominal interaction point (IP) in the centre of the detector and the z-axis along the beam pipe. The x-axis points from the IP to the centre of the LHC ring, and the y-axis points upwards. Cylindrical coordinates (r, ϕ) are used in the transverse plane, ϕ being the azimuthal angle around the z-axis. The pseudorapidity is defined in terms of the polar angle θ as $\eta = -\ln\tan(\theta/2)$. The angular distance between two physics objects is measured in units of $\Delta R \equiv \sqrt{(\Delta\eta)^2 + (\Delta\phi)^2}$.

JHEP06(2023)082

Simulated signal and background events were produced with various Monte Carlo (MC) event generators, processed through the full ATLAS detector simulation [20] using GEANT4 [21], and then reconstructed with the same procedure as is used for data.

The effect of multiple pp interactions in the same and neighbouring bunch crossings (referred to as pile-up) was modelled by overlaying the signal and background MC samples of simulated hard-scattering events with inelastic pp events generated with PYTHIA 8.186 [22] using the NNPDF2.3LO set of parton distribution functions (PDF) [23] and the A3 set of tuned parameters [24].

The signal $Z(\nu\bar{\nu})\gamma jj$ EWK events, including samples with non-zero aQGC parameters as well as interference between $Z(\nu\bar{\nu})\gamma jj$ EWK and QCD production and background $W(\ell\nu)\gamma jj$ EWK and $t\bar{t}\gamma jj$ events, were generated using MADGRAPH5_AMC@NLO at leading order (LO) in both QCD and QED, interfaced to the PYTHIA 8 [25] parton shower model. The decays of bottom and charm hadrons were simulated using the EVTGEN [26] program. Non-zero aQGC samples were generated for linear and quadratic BSM terms of the process amplitude for each effective field theory (EFT) operator considered.

For the signal $Z(\nu\bar{\nu})\gamma jj$ EWK sample, the next-to-leading-order (NLO) QCD corrections were produced with VBFNLO 2.7.1 [27], taking into account the m_{jj} dependence for consequent reweighting of MADGRAPH5_AMC@NLO result; the average value of the corrections is close to 1. The scale variations from VBFNLO for the NLO QCD process are used instead of those from the LO MADGRAPH5_AMC@NLO sample. EWK samples with an alternative parton shower model are obtained using HERWIG 7.13 [28, 29] instead of PYTHIA 8 and used for the evaluation of that systematic uncertainty.

The $V\gamma$ and V+jets QCD backgrounds, prompt single-photon (γjj) and multijet (jj) events, including $Z(\nu\bar{\nu})\gamma jj$, $W(\ell\nu)\gamma jj$, $Z(\ell\bar{\ell})\gamma jj$, $W(e\nu)jj$, $Z(\nu\bar{\nu})jj$ and $Z(e\bar{e})$ production, were generated using the SHERPA [30] generator. Matrix elements at NLO and LO QCD accuracy were matched and merged with the SHERPA parton shower based on Catani–Seymour dipole factorisation [31, 32] using the MEPS@NLO prescription [33–36]. The virtual QCD corrections for the matrix elements at NLO accuracy were provided by the OPENLOOPS library [37–39]. The samples using the NNPDF3.0NNLO [40] PDF set were normalised to the next-to-next-to-leading-order (NNLO) prediction [41].

An alternative $Z\gamma jj$ QCD sample was generated using MADGRAPH5_AMC@NLO 2.3.3 [42] at NLO interfaced to the PYTHIA 8.212 parton shower model. The merging procedure in the event generation was performed using the FxFx scheme [43].

Single-top or single-anti-top s-channel production was modelled using the POWHEG BOX v2 [44–47] generator, which provides matrix elements at NLO in the strong coupling constant in the five-flavour scheme with the NNPDF3.0NLO [40] PDF set. The events were interfaced with PYTHIA 8 using the NNPDF2.3LO PDF set. The decays of bottom and charm hadrons were simulated using the EVTGEN program.

The details of the matrix element generator, parton shower and parameter values (tune), PDF choice, and cross-section order for the processes mentioned above are listed in table 1.

JHEP06(2023)082

Physics process	Generator	Parton shower	Cross-section order in pQCD	Tune	PDF set
$Z(\nu\bar{\nu})\gamma jj$ EWK, $W(\ell\nu)\gamma jj$ EWK	MadGraph5_aMC@NLO 2.6.2 [48]	Pythia 8.235	LO, K-factor to NLO	A14 [49]	NNPDF2.3lo
$Z\gamma jj$ interference, aQGC	MadGraph5_aMC@NLO 2.6.7	Pythia 8.244	LO	A14	NNPDF2.3lo
Alternative $Z(\nu\bar{\nu})\gamma jj$ EWK & $W(\ell\nu)\gamma jj$ EWK	MadGraph5_aMC@NLO 2.6.2	Herwig 7.13	LO	A14	NNPDF2.3lo
$t\bar{t}\gamma jj$	MadGraph5_aMC@NLO 2.3.3	Pythia 8.212	LO, K-factor to NLO	A14	NNPDF2.3lo
Alternative $Z(\nu\bar{\nu})\gamma jj$	MadGraph5_aMC@NLO 2.3.3	Pythia 8.212	NLO	A14	NNPDF2.3lo
$Z(\nu\bar{\nu})\gamma jj$, $W(\ell\nu)\gamma jj$, $Z(\ell\bar{\ell})\gamma jj$	Sherpa 2.2.2	Sherpa 2.2.2	NLO	default	NNPDF3.0nnlo [40]
$W(e\nu)jj$, $W(\tau\nu)jj$, $Z(\nu\bar{\nu})jj$, $Z(e\bar{e})$	Sherpa 2.2.1	Sherpa 2.2.1	NLO	default	NNPDF3.0nnlo
γjj	Sherpa 2.1	Sherpa 2.1	LO, K-factor to NLO	default	CT10nlo [50]
jj	Sherpa 2.1.1	Sherpa 2.1.1	LO	default	CT10nlo
tjj, $t\bar{t}jj$	Powheg Box v2	Pythia 8.230	NLO	A14	NNPDF3.0nlo, NNPDF2.3lo

Table 1. Simulated signal and background event samples used in the analysis with the corresponding matrix element and parton shower generators, cross-section order in perturbative QCD (pQCD) used to normalise the event yield, underlying-event tune and PDF set. Where indicated the NLO cross section is obtained with K-factors.

4 Event reconstruction and selection

Candidate $Z(\nu\bar{\nu})\gamma jj$ events are selected by requiring the presence of a highly energetic photon, high missing transverse momentum and two jets. The lowest-threshold unprescaled single-photon trigger was chosen in order to select a high-energy phase-space region, which is sensitive to aQGC. This trigger requires a transverse energy $E_{\mathrm{T}}^{\gamma} > 140$ GeV and applies a 'loose' photon identification criterion [51]. The trigger efficiency for the photon candidates reconstructed offline and passing the 'tight' identification selection is more than 98.5% [52].

4.1 Object reconstruction

Photons are reconstructed [53] from clusters of energy deposited in the ECAL and selected to pass $|\eta| < 2.37$ and $E_{\mathrm{T}}^{\gamma} > 150$ GeV requirements. Clusters that are matched to one or two tracks originating from a conversion vertex are classified as converted photon candidates, whereas clusters without a matching track or reconstructed conversion vertex in the ID are classified as unconverted photon candidates. Electron candidates are reconstructed [53] from ECAL energy clusters and matched to a track reconstructed in the ID. They are required to have $|\eta| < 2.47$ and transverse momentum $p_{\mathrm{T}} > 7$ GeV. Both the photon and electron candidates must be outside of the calorimeter barrel/endcap transition region ($1.37 < |\eta| < 1.52$).

Muons are reconstructed [54] from tracks in the MS matched to a corresponding track in the ID (referred to as 'combined muons'). The combined track is required to have $p_{\mathrm{T}} > 7$ GeV and $|\eta| < 2.7$. Electron and muon tracks are required to originate from the primary vertex.[2] The transverse impact parameter significance[3] is required to be less than 5 and 3, respectively, for electrons and muons. The longitudinal impact parameter[4] must be less than 0.5 mm for both the electrons and muons.

[2]The primary vertex is identified as the vertex with the highest scalar sum of the squared transverse momenta in the event.

[3]The transverse impact parameter significance is defined as $|d_0|/\sigma(d_0)$, where d_0 is the distance of closest approach of e or μ to the primary vertex in the transverse plane with an uncertainty $\sigma(d_0)$.

[4]The longitudinal impact parameter is equal to $|z_0 \cdot \sin\theta|$, where z_0 is the difference between the value of the z coordinate of the point on the track at which d_0 is defined and the longitudinal position of the primary vertex.

JHEP06(2023)082

Photons and electrons are required to meet identification criteria based on their shower shapes in the ECAL, the amount of energy leaked into the hadronic calorimeter, and ID tracking information. The 'tight' photon identification criterion corresponding to passing all the requirements on shower shape variables is used in the analysis. The identification efficiency for the 'tight' photons is greater than 88% in Run 2 [53]. 'Loose' photons are selected in order to model jets misidentified as photons for the data-driven background estimation methods described in section 5. Electron candidates are required to satisfy the 'loose' electron identification criterion [53]. The 'medium' identification requirement is used for muon candidates [54].

Photons must satisfy the 'tight' isolation criterion [53], thereby fulfilling two requirements. Firstly, the sum of the transverse energies (at the electromagnetic energy scale) of positive-energy topological clusters located within a distance $\Delta R = 0.4$ of the photon candidate must be less than $0.022 \cdot E_{\mathrm{T}}^{\gamma} + 2.45$ GeV. Secondly, the scalar sum of the transverse momenta of the tracks located within a distance $\Delta R = 0.2$ of the photon candidate must be less than $0.05 \cdot E_{\mathrm{T}}^{\gamma}$. The 'loose' isolation requirement is imposed on electrons and muons [53, 54].

To suppress the beam-induced background [55], the z-axis coordinate pointed to by the photon candidate is required to be less than 250 mm from the identified primary vertex.

Jets are reconstructed from topological clusters in the calorimeters using the anti-k_t algorithm [56, 57] with a radius parameter of $R = 0.4$ and are required to have $p_{\mathrm{T}} > 20$ GeV. Jets are fully calibrated using the jet energy scale derived from 13 TeV data and simulation [58] and corrected for pile-up effects [59]. To suppress jets originating from pile-up, jets with $|\eta| < 2.5$ and $20 < p_{\mathrm{T}} < 120$ GeV must satisfy the 'medium' identification requirement placed on the jet vertex tagger (JVT) output [60]. The forward pile-up jet vertex tagger (fJVT) [61], which can be applied to jets with $2.5 < |\eta| < 4.5$ and $20 < p_{\mathrm{T}} < 120$ GeV, causes marginal changes, so it is not performed. The selected jets are required to have $p_{\mathrm{T}} > 50$ GeV and $|\eta| < 4.5$.

The missing transverse momentum $\vec{p}_{\mathrm{T}}^{\,\mathrm{miss}}$ is computed as the negative vector sum of the transverse momenta of candidate leptons with $p_{\mathrm{T}} > 7$ GeV, photons with $p_{\mathrm{T}} > 10$ GeV, jets with $p_{\mathrm{T}} > 20$ GeV, and tracks from the primary vertex not associated with any physics objects (the 'soft term') [62]. The quantity $E_{\mathrm{T}}^{\mathrm{miss}}$ is defined as the magnitude of $\vec{p}_{\mathrm{T}}^{\,\mathrm{miss}}$ and is used as a measure of the total transverse momentum of particles not registered by the detector.

Possible double counting of contributions from reconstructed particles is avoided by applying an ambiguity resolution procedure. The objects are removed in the following order: first, an electron lying within a $\Delta R = 0.1$ cone around a muon, then a selected jet without any JVT requirement lying within $\Delta R = 0.3$ of a photon, muon, or electron, and, finally, a photon lying within $\Delta R = 0.4$ of either a muon or an electron.

4.2 Region definitions

The $Z\gamma$ inclusive region requires events with exactly one 'tight' isolated photon with transverse energy $E_{\mathrm{T}}^{\gamma} > 150$ GeV and at least two jets. Selected events must also have

JHEP06(2023)082

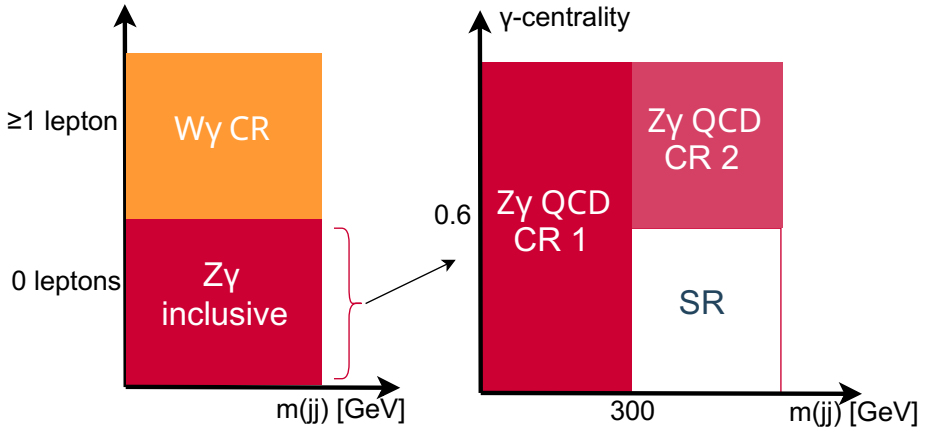

Figure 2. Definition of the regions used in the analysis.

$E_{\mathrm{T}}^{\mathrm{miss}} > 120$ GeV and calorimeter-measured $E_{\mathrm{T}}^{\mathrm{miss}}$ significance[5] greater than 12. An angular separation between both the leading (highest-p_{T}) and subleading (second-highest-p_{T}) jets $j_{1,2}$ and $\vec{p}_{\mathrm{T}}^{\mathrm{miss}}$ of $|\Delta\phi(j_{1/2}, \vec{p}_{\mathrm{T}}^{\mathrm{miss}})| > 0.3$ is also required. These criteria reduce the number of background events characterised by $E_{\mathrm{T}}^{\mathrm{miss}}$ arising from instrumental sources or poorly reconstructed physics objects (fake $E_{\mathrm{T}}^{\mathrm{miss}}$), mainly due to the γjj process. A lepton veto, which discards events with any electron or muon candidate, is applied to reduce the contribution from $W(\ell\nu)\gamma jj$ and $Z(\ell\bar{\ell})\gamma jj$ backgrounds. An azimuthal angle requirement $|\Delta\phi(\gamma, \vec{p}_{\mathrm{T}}^{\mathrm{miss}})| > 0.4$ significantly decreases the $W(e\nu)jj$ background. Finally, a restriction on the soft term of $\vec{p}_{\mathrm{T}}^{\mathrm{miss}}$ reconstructed from ID tracks, $p_{\mathrm{T}}^{\mathrm{SoftTerm}} < 16$ GeV, is effective against most backgrounds.

The $W\gamma$ control region (CR) requires events with at least one lepton. All other selection criteria are the same as for the $Z\gamma$ inclusive region.

The $Z\gamma$ inclusive region is divided into three subregions as shown in figure 2. The signal region (SR) is required to have $m_{jj} > 300$ GeV and γ-centrality[6] < 0.6, where m_{jj} is defined as the invariant mass of the two jets with the highest values of p_{T} in the event. The $Z\gamma$ QCD CR 1 requires events with $m_{jj} < 300$ GeV; it is used to estimate the $Z(\nu\bar{\nu})\gamma jj$ QCD background yield. The $Z\gamma$ QCD CR 2 has the same selection criteria as the SR but requires events with γ-centrality > 0.6; it is used to check for possible m_{jj} mismodelling. The values of the requirements are chosen to maximise the number of events and the purity of the targeted process in each region.

[5] $E_{\mathrm{T}}^{\mathrm{miss}}$ significance is calculated as $|\vec{p}_{\mathrm{T}}^{\mathrm{miss}}|^2 / \left(\sigma_{\mathrm{L}}^2 \left(1 - \rho_{\mathrm{LT}}^2\right)\right)$, where σ_{L} is the total variance in the direction longitudinal to the $E_{\mathrm{T}}^{\mathrm{miss}}$, and ρ_{LT} is the correlation coefficient of the longitudinal (L) and transverse (T) measurements [63].

[6] Photon centrality relative to the two jets with the highest p_{T} values in the event is defined as γ-centrality $= \left|\frac{y(\gamma) - 0.5[y(j_1)+y(j_2)]}{y(j_1)-y(j_2)}\right|$, where $y = 0.5 \times \ln[(E+p_z)/(E-p_z)]$ is the rapidity of the objects (p_z is the z-component of the momentum of a particle).

JHEP06(2023)082

5 Background estimation

The main background for the $Z\gamma jj$ EWK process is QCD production of $Z(\nu\bar{\nu})\gamma jj$. This background constitutes 36% of the total predicted event yield in the SR.[7] It is estimated from a simultaneous fit of the MC distributions to data in the control regions described in section 4. The fit procedure is detailed in section 7.

Other well-modelled backgrounds [9, 64, 65] arise from $W(\ell\nu)\gamma jj$ QCD and EWK production, and production of $t\bar{t}\gamma jj$ with semileptonic or fully leptonic decays. They contribute 25%, 7% and 6% to the total predicted event yield in the SR repectively. Their distribution shapes are taken from MC predictions and their normalisation is obtained from the simultaneous fit. Varying the ratio of $W(\ell\nu)\gamma jj$ to $t\bar{t}\gamma jj$ contributions has negligible impact on the fit result.

The minor background from $Z(\ell\bar{\ell})\gamma jj$ production is estimated from MC simulation and without normalisation via the fit (it is less than 1% of the predicted event yield in the SR). In all these processes except $Z(\nu\bar{\nu})\gamma jj$, the leptons are either not reconstructed or they are τ-leptons which decay into hadrons.

Background processes with object misidentification or incorrect energy measurement are not well modelled by the MC simulation, and so they are estimated from data. There are three such background processes: $e \to \gamma$ misidentification, $E_{\mathrm{T}}^{\mathrm{miss}}$ mismeasurement, and $j \to \gamma$ misidentification. They respectively contribute 6%, 5.5% and 2% to the total predicted event yield in the SR. These backgrounds are included in the simultaneous fit, with the normalisation estimated from data.

The sources of the $e \to \gamma$ misidentification background are mainly processes with a W boson decaying leptonically, which are $W(e\nu)jj$, tjj, and $t\bar{t}jj$ production. At high energies, such misidentification mainly occurs when a prompt electron is mistaken for a prompt photon, e.g. if an electron's track is not reconstructed in the ID. The $e \to \gamma$ misidentification rate ($f_{e\to\gamma}$) is estimated from data using a variation of the tag-and-probe method (e.g. in ref. [66]), in which it is assumed that $e\gamma$ pairs with invariant mass near the Z boson mass contain an electron or positron misidentified as a photon. The probe photon is selected in the same way as the SR photon, while the probe electron is selected with a method that is as close as possible to the selection of the SR photon. In this case, $f_{e\to\gamma}$ can be estimated as the ratio of the number of events containing $e\gamma$ to the number containing e^+e^- tag-and-probe pairs in the Z-peak region after subtraction of the Drell–Yan background. The subtraction is performed using extrapolation of an exponential polynomial fit of the Drell–Yan background outside the Z-peak region. The measured $f_{e\to\gamma}$ ranges from 2% to 6.8% depending on photon η and E_{T}. The systematic uncertainty of the $f_{e\to\gamma}$ estimate ranges from 3.7% to 16%. It has three contributions, which are, listed in decreasing order of magnitude, the uncertainty from a check of the method's validity in $Z(ee)$ simulation, the uncertainty from the fit to estimate the background under the Z peak, and the choice of Z-peak region. The statistical uncertainty of $f_{e\to\gamma}$ ranges from 2.5% to 6.3%. The measured value of $f_{e\to\gamma}$ is then used to estimate the background yield. The corresponding

[7] The indicated percentages of background contributions are calculated using the predicted event yield after the fit described in section 7.

JHEP06(2023)082

$W(e\nu)jj$-enriched regions are built in data for the $W\gamma$ CR, the $Z\gamma$ inclusive region, the $Z\gamma$ QCD CR 1 and CR 2, and the SR, with a probe electron selected instead of a photon. The resulting event yields or distributions are multiplied by $f_{e\to\gamma}$, taking into account η and E_{T} dependencies. The total systematic uncertainty of the background estimate includes systematic and statistical uncertainties of the $f_{e\to\gamma}$ estimate and also the impurity of the probe-electron control region. According to MC simulations, the contamination consists of events with fake electrons from $j \to e$ misidentification and varies from less than 1% to 2% depending on the region; these values are taken as the systematic uncertainties. The total systematic uncertainty of the $e \to \gamma$ background estimate varies from 4.7% to 7.4%.

The mismeasured $E_{\mathrm{T}}^{\mathrm{miss}}$ in γ+jets production occurs when there is an incorrect measurement of the jet energy or when some of the jets are not reconstructed in the event. To estimate this background, a two-dimensional sideband (ABCD) method (e.g. see ref. [67]) based on the $E_{\mathrm{T}}^{\mathrm{miss}}$ significance and $p_{\mathrm{T}}^{\mathrm{SoftTerm}}$ discriminating variables is used. Region A corresponds to the $Z\gamma$ inclusive region. Orthogonal control regions B, C, and D are built by inverting either of the analysis selections on $E_{\mathrm{T}}^{\mathrm{miss}}$ significance or $p_{\mathrm{T}}^{\mathrm{SoftTerm}}$, or both. The discriminating variables are chosen to ensure that the correlation between them is small and to minimise leakage of signal events into the control regions. In this case, the relation between the numbers of background events in the ABCD regions is $N_{\mathrm{A}}/N_{\mathrm{B}} = N_{\mathrm{C}}/N_{\mathrm{D}}$. The background of γ+jets in the $Z\gamma$ inclusive region is estimated using the yields observed in the B, C, and D regions in the data, where contamination with non-γ+jets events is removed using either MC simulation or data-driven estimation. The correlation factor[8] is estimated from γ+jets MC events and is 1.09 ± 0.18; a value of 1 would indicate an absence of correlation. The statistical uncertainty of the fake-$E_{\mathrm{T}}^{\mathrm{miss}}$ background is assessed by independently varying the non-γ+jets backgrounds in the control regions by $\pm 1\sigma$. It results in a 44% uncertainty in this background estimate for the $Z\gamma$ inclusive region. The total systematic uncertainty is 32%. The dominant contribution (31%) is obtained by varying the correlation factor by its uncertainty. To obtain estimates of this background in the signal and control regions of the analysis (the $Z\gamma$ QCD CRs and $W\gamma$ CR), the distributions of m_{jj} and γ-centrality from the γ+jets MC events are used. They are found to be in agreement with data within the uncertainties, after subtraction of other backgrounds. The γ+jets MC events are used to model the shape of this background in the fit for the observable used for the cross-section extraction.

Background from $j \to \gamma$ misidentification arises mainly from Z boson production where the Z boson decays into a neutrino–antineutrino pair and from multijet production combined with fake $E_{\mathrm{T}}^{\mathrm{miss}}$. This background is also estimated using the ABCD method, with A region corresponding to the $Z\gamma$ inclusive region. The discriminating variables are those used in the photon isolation and ECAL shower-shape identification criteria. To construct the orthogonal regions, the SR requirement for the photon to satisfy the 'tight' identification criteria is replaced by a 'non-tight' requirement for the C and D regions, and the ECAL-based isolation criterion is inverted in the B and D regions. The 'non-tight'

[8]The correlation factor in MC is determined as $R = \frac{N_A \cdot N_D}{N_B \cdot N_C}$, where N_i is the number of background events in the corresponfing control region. In absence of correlation $R = 1$.

JHEP06(2023)082

photon candidate must fail at least one of the two shower shape selections [68] w_{s3},[9] and F_{side},[10] which are associated with the strip layer of the ECAL. These are chosen instead of other 'non-tight' variables because of their lower correlation with isolation variables used in the construction of the regions. In addition, the correlation factor obtained from $Z(\nu\bar{\nu})jj$ inclusive MC simulation and the one obtained from data agree best when using this 'non-tight' definition. The statistical uncertainty of the $j \to \gamma$ background is obtained in the same way as for the γ+jets background. The largest uncertainty in the background estimate is 52% for the $Z\gamma$ inclusive region. The dominant systematic uncertainty comes from variations of the control region definition[11] and is 18%, while the total is 19%. The $Z(\nu\bar{\nu})\gamma jj$ QCD MC sample is used as a template for the background in the fit and for the extrapolation to the signal and control regions of the analysis (these are the $Z\gamma$ QCD control regions and $W\gamma$ control region). The reason why the $Z(\nu\bar{\nu})\gamma jj$ QCD MC sample is used instead of the $Z(\nu\bar{\nu})jj$ inclusive MC sample is that far fewer events are selected from the latter; the distributions from these MC samples agree within their uncertainties.

Another background, due to pile-up, arises when the photon and Z boson are produced in different pp collisions in the same LHC bunch crossing. This background is estimated from the distribution of the longitudinal separation between the reconstructed primary vertex and the reconstructed coordinate of a photon's origin. Only converted photons are used since they have better z-coordinate resolution. This contribution has no significant effect on the overall background shape and is considered only as a systematic normalisation uncertainty of 1.9% in the fit.

6 Systematic uncertainties

Experimental sources of systematic uncertainty include uncertainties in the energy scale and resolution of jets, photons and electrons, in the scale and resolution of the muon momentum, and in the missing transverse momentum. Additional contributors to the experimental uncertainty are the uncertainties in the scale factors used to reproduce the trigger, reconstruction, identification and isolation efficiencies, and pile-up conditions measured in data. The uncertainty in the combined 2015–2018 integrated luminosity is 1.7% [18], obtained using the LUCID-2 detector [19] for the primary luminosity measurements.

The theoretical systematic uncertainties considered in this analysis are related to higher-order QCD corrections and our choice of PDF and value of the strong coupling constant α_s. The uncertainties due to higher-order QCD corrections are estimated by varying the renormalisation and factorisation scales by factors of one-half and two, and

[9] Front lateral width (3 strips) measures the shower width along η in the first layer of the electromagnetic calorimeter, using a total of three strip cells centred on the largest energy deposit. It is calculated as $w_{s3} = \sqrt{\frac{\Sigma E_i (i-i_{max})^2}{\Sigma E_i}}$. The index i is the strip identification number, i_{max} identifies the strip cell with the most energy, and E_i is the energy deposit in each strip cell.

[10] Front side energy ratio measures the lateral containment of the shower along the η direction. It is calculated as $F_{side} = \frac{E(\pm 3) - E(\pm 1)}{E(\pm 1)}$, where $E(\pm n)$ is the energy in the $\pm n$ strip cells around the one with the most energy.

[11] Variations consist in the choice of non-tight identification criteria and the choice of the energy gap between regions with normal and inverted isolation criteria.

JHEP06(2023)082

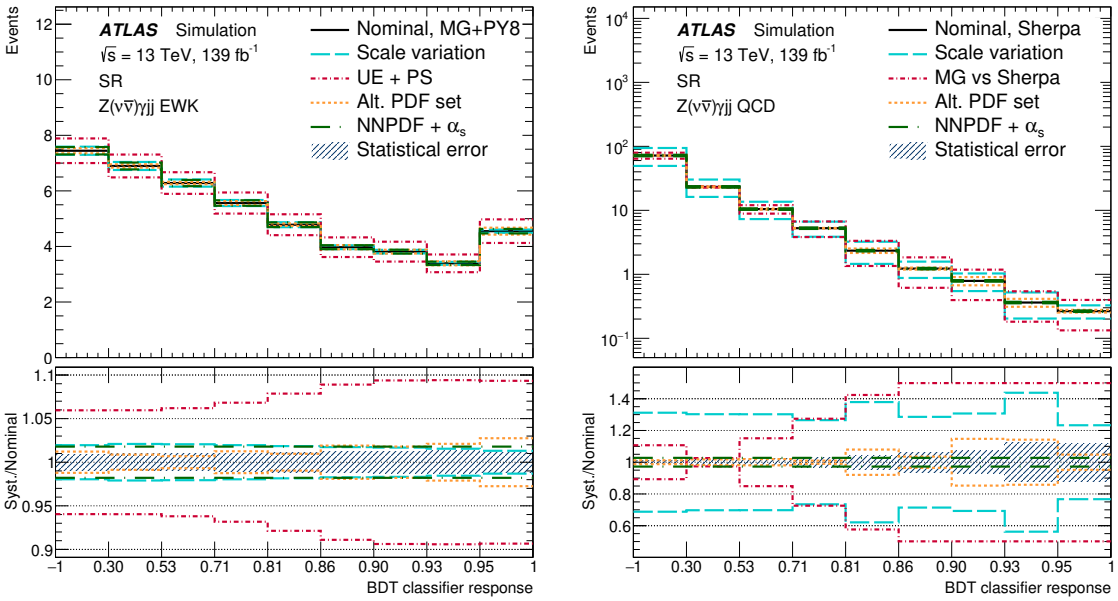

(a) (b)

Figure 3. These graphs indicate the effect of the main theory uncertainties, which are associated with the renormalisation and factorisation scales (dashed cyan), underlying event and parton showering (UE+PS) or generator choice (dash-dotted red), alternative PDF sets (dotted orange), combined NNPDF set variation and α_s uncertainty (loosely dash-dotted green). These are shown in the signal region for (a) the $Z(\nu\bar{\nu})\gamma jj$ EWK process and (b) the $Z(\nu\bar{\nu})\gamma jj$ QCD process. The BDT classifier response was remapped into equal width bins for better representation. The uncertainty band corresponds to the uncertainty due to the limited number of MC events.

ignoring the combinations that differ by a factor of four. The uncertainties due to the PDF and α_s choice are estimated using the PDF4LHC prescription [69]. Additionally, a global modelling uncertainty was evaluated using an alternative MC generator either for the matrix element generation, underlying event and parton showering or for only the last two of these. The alternative PDF sets and MC generators are described in section 3.

The signal selection uses a boosted decision tree (BDT). The signal-to-background ratio is expected to increase at high values of the BDT classifier as is described in section 7. The effect of the theoretical systematic uncertainties on the $Z(\nu\bar{\nu})\gamma jj$ EWK and $Z(\nu\bar{\nu})\gamma jj$ QCD processes, versus BDT classifier response, is shown in figure 3.

The yield of the interference between the $Z(\nu\bar{\nu})\gamma jj$ EWK signal and QCD background is estimated to be small (5.8% of the total signal yield in the SR) so it is not included as a part of the electroweak signal in the fit. Instead, the signal is represented by the pure electroweak process, and the directly generated interference contribution is taken as an extra signal uncertainty.

Additional uncertainties related to data-driven background estimates are also considered. Systematic uncertainties are assigned to the normalisation of the backgrounds from $e \to \gamma$ misidentification, $j \to \gamma$ misidentification, incorrect $E_{\mathrm{T}}^{\mathrm{miss}}$ measurement, and the

JHEP06(2023)082

combination of a Z boson and a photon from different pp collisions (pile-up background), with values corresponding to those described in section 5.

Mismodelling of the m_{jj} distribution is observed in the $Z\gamma$ QCD CR 2 (see figure 4(b), where the prediction-to-data ratio has $\chi^2/N_{\text{df}} = 8.2/7$ and a p-value $= 0.31$) and could have a similar impact in the SR. Since the $Z(\nu\bar{\nu})\gamma jj$ QCD and $W(\ell\nu)\gamma jj$ QCD processes are the dominant ones in this region (contributing 45% and 31% of the total predicted event yield, respectively) and the $W(\ell\nu)\gamma jj$ QCD process is shown to be accurately modelled in the $W\gamma$ CR (see figure 4(c)), the mismodelling is attributed to the $Z(\nu\bar{\nu})\gamma jj$ QCD process. Due to the similarities between these two processes (being produced by the same MC generator and having final-state kinematical properties that differ only because of the final-state boson) and the fact that the $W\gamma$ CR has data in all of the m_{jj} and γ-centrality spectra bins, the $Z(\nu\bar{\nu})\gamma jj$ QCD modelling in the SR was checked with the $W(\ell\nu)\gamma jj$ QCD process in the analogous part of the $W\gamma$ CR. This validates the modelling of $Z(\nu\bar{\nu})\gamma jj$ QCD in the SR to the level of agreement between the $Z(\nu\bar{\nu})\gamma jj$ QCD and $W(\ell\nu)\gamma jj$ QCD processes, and to the level of agreement between the $W(\ell\nu)\gamma jj$ QCD process and the data. The discrepancies are used to assign two systematic uncertainties to the $Z(\nu\bar{\nu})\gamma jj$ QCD contribution in the SR, resulting in 15% and 23% relative uncertainties in the total event yield, respectively.

7 Signal extraction procedure and results

A BDT classifier created with the TMVA [70] package is used to separate the signal from the background processes described in section 5. It is trained in the $Z\gamma$ inclusive region. Due to the low number of events in the $Z\gamma$ inclusive region, the γ+jets, $Z(\ell\bar{\ell})\gamma$ and Zj, and multijet (jj) backgrounds are not used to train the classifier. In order to utilise the full set of simulated events, two classifiers are created and trained on two statistically independent samples. The classifier trained on one sample is applied to the other, and the final response distribution is built by combining the responses of these two classifiers. The following variables are used to create the classifier: m_{jj}, $\Delta y(j_1, j_2)$, $E_{\text{T}}^{\text{miss}}$, p_{T}-balance,[12] $\eta(j_2)$, $p_{\text{T}}(j_1)$, $\eta(\gamma)$, p_{T}-balance (reduced),[13] N_{jets}, $\sin(|\Delta\varphi(j_1, j_2)/2|)$ and $\Delta y(j_1, \gamma)$. This is the smallest set of variables that gives the classifier sufficient separation power. Although the γ-centrality provides as much separation power as m_{jj} or $\Delta y(j_1, j_2)$, it was not used in the classifier because this allows the creation of an independent $Z\gamma$ QCD CR 2 that was used to check the modelling of the m_{jj} distribution.

To extract the $Z(\nu\bar{\nu})\gamma jj$ EWK cross section, a binned maximum-likelihood fit [71] is performed using the BDT classifier response distribution in the SR and the m_{jj} distributions in the $Z\gamma$ QCD CRs 1 and 2 and the $W\gamma$ CR; this combination uses 31 bins. Three free parameters are introduced in the combined fit: a signal strength parameter, $\mu_{Z\gamma\text{EWK}}$, and two normalisation factors for the main background sources. The first, $\mu_{Z\gamma\text{QCD}}$, is used to scale the $Z(\nu\bar{\nu})\gamma jj$ QCD process yield, while $\mu_{W\gamma}$ is used to scale the yields of the $W(\ell\nu)\gamma jj$ QCD, $W(\ell\nu)\gamma jj$ EWK and $t\bar{t}\gamma jj$ processes because of their similar final states.

[12] The p_{T}-balance $= \frac{|\vec{p}_{\text{T}}^{\,\text{miss}} + \vec{p}_{\text{T}}^{\,\gamma} + \vec{p}_{\text{T}}^{\,j1} + \vec{p}_{\text{T}}^{\,j2}|}{E_{\text{T}}^{\text{miss}} + E_{\text{T}}^{\gamma} + p_{\text{T}}^{j1} + p_{\text{T}}^{j2}}$.

[13] The p_{T}-balance (reduced) $= \frac{|\vec{p}_{\text{T}}^{\,\gamma} + \vec{p}_{\text{T}}^{\,j1} + \vec{p}_{\text{T}}^{\,j2}|}{E_{\text{T}}^{\gamma} + p_{\text{T}}^{j1} + p_{\text{T}}^{j2}}$.

JHEP06(2023)082

Each source of systematic uncertainty is implemented in the likelihood function as a nuisance parameter (NP) with a Gaussian constraint. All instrumental uncertainties, as well as the pile-up background uncertainty, are treated as correlated between the processes and regions. Almost all of the other uncertainties are treated as correlated between regions. The exceptions are the scale uncertainties for all of the processes and the modelling uncertainties of the $Z(\nu\bar{\nu})\gamma jj$ QCD and $W(\ell\nu)\gamma jj$ QCD processes. All scale uncertainties are uncorrelated between the regions. The modelling uncertainties are separated into two groups: one correlated between all of the CRs and one for the SR. This conservative approach avoids unnecessary constraints upon systematic uncertainties coming from the differences in the MC generators.

To account for the effect of the limited size of the simulated samples, an uncertainty with a Poissonian constraint is introduced for bins with a relative statistical uncertainty higher than 5%. The signal strength, background normalisation coefficients and yields for all of the processes are estimated in the fit to the observed data in the signal and control regions.

The observed significance is estimated by setting $\mu_{Z\gamma\mathrm{EWK}} = 0$ and performing a background-only fit to the data in all of the regions so as to determine the probability of rejecting the background-only hypothesis. In this approach uncertainties that only affect the signal process (i.e. theoretical uncertainties and the $Z(\nu\bar{n}u)jj$ EWK/QCD interference) have no effect on the significance calculation. The expected significance is estimated by fitting the artificial Asimov dataset in the same way. Such a dataset is constructed by modifying the predicted values with the normalisation coefficients and NPs obtained in the fit in the CRs while assuming no signal is present [72].

The signal strength is measured to be:

$$\mu_{Z\gamma\mathrm{EWK}} = 0.78^{+0.25}_{-0.23}\ (\mathrm{stat.})^{+0.21}_{-0.17}\ (\mathrm{syst.}).$$

The observed (expected) significance of the result is 3.2σ (3.7σ). The $\mu_{Z\gamma\mathrm{QCD}}$ and $\mu_{W\gamma}$ normalisation coefficients are measured to be $1.21^{+0.37}_{-0.31}$ and $1.02^{+0.22}_{-0.17}$, respectively, signifying agreement with the predicted yields within the uncertainties.

The predicted fiducial cross section is computed in the phase space defined in table 2. The definition of the fiducial phase space closely follows the detector-level selections, using photons, electrons, muons, $E_{\mathrm{T}}^{\mathrm{miss}}$ and jets at the particle level. These stable final-state particles (with proper decay length $c\tau > 10$ mm) are produced in the hard scatter; this includes those that are the products of hadronisation. Thus they are reconstructed in simulation, prior to their interactions with the detector. The leptons used in the veto are reconstructed at the particle level, with a correction for fully recovered final-state radiation applied. No requirement is placed on the $E_{\mathrm{T}}^{\mathrm{miss}}$ significance or $p_{\mathrm{T}}^{\mathrm{SoftTerm}}$ due to the complexity of defining these variables at particle level; however, the detector-level $E_{\mathrm{T}}^{\mathrm{miss}}$ requirement is applied to the particle-level $E_{\mathrm{T}}^{\mathrm{miss}}$, which corresponds to the E_{T} of the dineutrino system. All the other kinematic selection requirements are the same as those at detector level in section 4.2. The fiducial region selection efficiency is 33%. The fiducial cross section was predicted with MadGraph5_aMC@NLO (interfaced with Pythia) at leading order, with next-to-leading-order QCD corrections and scale uncertainties computed with

JHEP06(2023)082

Selections	Cut value
$E_{\mathrm{T}}^{\mathrm{miss}}$	$> 120\,\mathrm{GeV}$
E_{T}^{γ}	$> 150\,\mathrm{GeV}$
Number of isolated photons	$N_{\gamma} = 1$
Photon isolation	$E_{\mathrm{T}}^{\mathrm{cone40}} < 0.022 p_{\mathrm{T}} + 2.45\,\mathrm{GeV}$, $p_{\mathrm{T}}^{\mathrm{cone20}}/p_{\mathrm{T}} < 0.05$
Number of jets	$N_{\mathrm{jets}} \geq 2$ with $p_{\mathrm{T}} > 50\,\mathrm{GeV}$
Overlap removal	$\Delta R(\gamma, \mathrm{jet}) > 0.3$
Lepton veto	$N_e = 0$, $N_{\mu} = 0$
$\lvert\Delta\phi(\gamma, \vec{p}_{\mathrm{T}}^{\mathrm{miss}})\rvert$	> 0.4
$\lvert\Delta\phi(j_1, \vec{p}_{\mathrm{T}}^{\mathrm{miss}})\rvert$	> 0.3
$\lvert\Delta\phi(j_2, \vec{p}_{\mathrm{T}}^{\mathrm{miss}})\rvert$	> 0.3
m_{jj}	$> 300\,\mathrm{GeV}$
γ-centrality	< 0.6

Table 2. Fiducial region definition.

VBFNLO. Its value is

$$\sigma_{Z\gamma\mathrm{EWK}}^{\mathrm{pred}} = 0.98 \pm 0.02\ (\mathrm{stat.}) \pm 0.09\ (\mathrm{scale}) \pm 0.02\ (\mathrm{PDF})\ \mathrm{fb}.$$

Combined with the measured signal strength, it results in an observed fiducial cross section of

$$\sigma_{Z\gamma\mathrm{EWK}} = 0.77^{+0.34}_{-0.30}\ \mathrm{fb} = 0.77^{+0.25}_{-0.23}\ (\mathrm{stat.})^{+0.22}_{-0.18}\ (\mathrm{syst.})\ \mathrm{fb}.$$

Table 3 shows the observed and expected event yields of the signal and backgrounds in the SR and CRs after the fit is performed. The post-fit m_{jj} and BDT classifier response distributions are shown in figure 4, and the summary plot for all of the regions is shown in figure 5.

The breakdown of the impact of groups of systematic uncertainties on the cross-section measurement is shown in table 4, with the theoretical uncertainties of the electroweak signal and the $Z(\nu\bar{\nu})\gamma jj$ QCD background having the largest impact.

8 Combination with previous ATLAS measurement

To increase the sensitivity, the measurement of electroweak $Z(\nu\bar{\nu})\gamma jj$ production presented in this paper is combined with the measurement from the previously published ATLAS observation of this process [7]. The analyses are statistically independent because their phase-space regions are orthogonal in E_{T}^{γ}. This analysis requires $E_{\mathrm{T}}^{\gamma} > 150$ GeV, while the previous ATLAS analysis requires $15 < E_{\mathrm{T}}^{\gamma} < 110$ GeV.

The combined $Z(\nu\bar{\nu})\gamma jj$ EWK signal strength and its significance are extracted from a simultaneous profile likelihood fit. The fit includes all signal and control regions of both analyses and all corresponding systematic uncertainties. Various correlation schemes of jet energy and theoretical QCD scale uncertainties were tested and found to have negligible effect on the combined result. The observed (expected) significance of the combined result

JHEP06(2023)082

	$W\gamma$ CR	$Z\gamma$ QCD CR 1	$Z\gamma$ QCD CR 2	Signal region
$Z(\nu\bar{\nu})\gamma jj$ EWK	0.108 ± 0.028	11.0 ± 4.3	4.0 ± 2.2	37 ± 14
$Z(\nu\bar{\nu})\gamma jj$ QCD	1.04 ± 0.46	394 ± 84	143 ± 32	133 ± 39
$W(\ell\nu)\gamma jj$ QCD	425 ± 63	237 ± 71	76 ± 24	91 ± 30
$W(\ell\nu)\gamma jj$ EWK	63 ± 12	14.3 ± 2.7	4.5 ± 1.2	24.6 ± 4.9
$W(e\nu)jj$, tjj, $t\bar{t}jj$	39.8 ± 2.5	70.1 ± 4.1	17.9 ± 1.3	22.5 ± 1.5
$t\bar{t}\gamma jj$	193 ± 57	57 ± 20	9.1 ± 3.4	21.3 ± 7.6
γjj	4.8 ± 7.4	52 ± 36	8 ± 11	20 ± 17
Zj, jj	0.06 ± 0.66	20 ± 14	5.9 ± 6.9	6.6 ± 7.8
$Z(\ell\bar{\ell})\gamma jj$	8.6 ± 2.5	6.8 ± 2.0	2.04 ± 0.95	2.2 ± 1.3
Total	735 ± 30	863 ± 54	271 ± 25	357 ± 30
Data	737	849	268	356

Table 3. Observed and expected event yields for the signal and all of the background processes considered in this analysis after the fit to the data in all of the regions. The uncertainty in the expected yield is the combination of statistical and systematic uncertainties obtained in the fit. The individual uncertainties can be correlated and do not necessarily add in quadrature to equal the total expected uncertainty.

Source of uncertainty	$\Delta\sigma/\sigma$ [%]
Experimental	
Jets	-3.2 / $+3.4$
Electrons and photons	-0.3 / $+1.7$
Muons	-0.4 / $+0.5$
$E_{\mathrm{T}}^{\mathrm{miss}}$	-1.8 / $+2.2$
Pile-up modelling	-1.7 / $+3.2$
Trigger efficiency	-0.9 / $+2.1$
Luminosity	-1.2 / $+2.6$
Theory	
$Z(\nu\bar{\nu})\gamma jj$ EWK/QCD interference	-0.6 / $+2.6$
$Z(\nu\bar{\nu})\gamma jj$ EWK process	-6 / $+12$
$Z(\nu\bar{\nu})\gamma jj$ QCD process	-15 / $+16$
Other processes	-5.3 / $+7.7$
Other sources	
Data-driven backgrounds	-0.9 / $+1.2$
Pile-up background	-1.2 / $+2.6$
$Z(\nu\bar{\nu})\gamma jj$ QCD m_{jj} modelling	-4.4 / $+4.4$

Table 4. Impact of different components of the systematic uncertainty on the measured cross section, without taking into account the correlations. The impact is calculated by fixing the value of the corresponding nuisance parameters to the values obtained in the fit used to measure the cross section, performing the fit, estimating the signal strength uncertainty, subtracting its square from the square of the nominal uncertainty, and calculating the square root.

JHEP06(2023)082

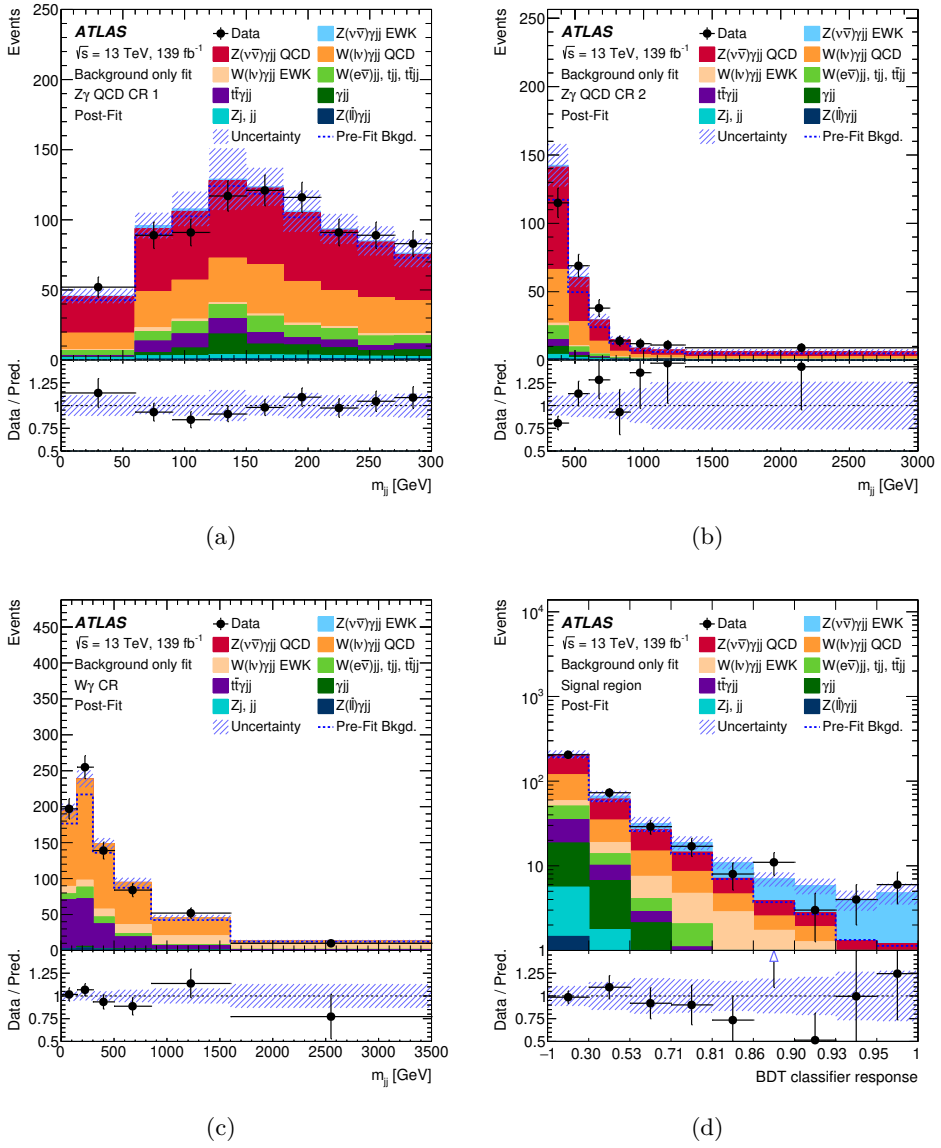

Figure 4. The m_{jj} distributions for the (a) $Z\gamma$ QCD CR 1, (b) $Z\gamma$ QCD CR 2, and (c) $W\gamma$ CR, and the BDT classifier response distribution for the (d) SR after the fit in all regions. The BDT classifier response was remapped into equal-width bins for better representation. The dashed line shows the total background distribution before the fit. The vertical error bars on the data points correspond to the data's statistical uncertainty. Overflows are included in the last bin. The lower panel shows the ratio of observed to expected event yields. The uncertainty band corresponds to the combination of the statistical and systematic uncertainties obtained in the fit.

JHEP06(2023)082

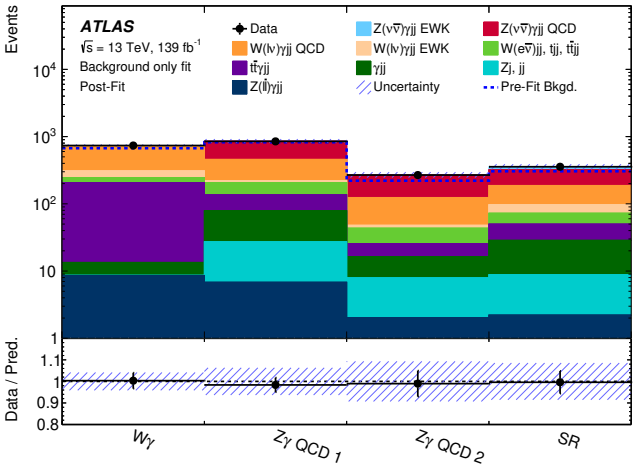

Figure 5. Summary of the yield for processes in all regions, after the fit over all regions. The dashed line shows the total background distribution before the fit. The vertical error bars on the data points correspond to the data's statistical uncertainty. The lower panel shows the ratio of observed to expected event yields. The uncertainty band corresponds to the combination of the statistical and systematic uncertainties obtained in the fit.

	Value		
POI	Current analysis	Ref. [7]	Combination
$\mu_{Z\gamma\text{EWK}}$	0.78 ± 0.33	1.03 ± 0.25	0.96 ± 0.19
$\mu_{Z\gamma\text{QCD}}$	1.21 ± 0.37	1.02 ± 0.41	1.17 ± 0.27
$\mu_{W\gamma}$	1.02 ± 0.22	1.01 ± 0.20	1.01 ± 0.13

Table 5. Fitted POI values for this analysis, the previous ATLAS analysis, and their combination. The second and third columns present the values obtained in the individual analyses. The fourth column presents the values obtained in the combination.

with $\mu_{Z\gamma\text{EWK}}$ as the parameter of interest (POI) is 6.3σ (6.6σ). The fitted values of the signal strength ($\mu_{Z\gamma\text{EWK}}$) and background normalisations ($\mu_{Z\gamma\text{QCD}}$ and $\mu_{W\gamma}$) are listed in table 5.

The difference in $\mu_{Z\gamma\text{EWK}}$ for the two analyses in combination is due to the lower data statistics in the signal region of the current analysis. The difference in $\mu_{Z\gamma\text{QCD}}$ for two analyses in combination is due to the different renormalisation and refactorisation scale correlation schemes used in the individual analyses. The most conservative correlation scheme that results in the highest expected uncertainty of the POI is used for both analyses to obtain the combination result.

The observed cross section using the combined signal strength is 9.2 ± 2.0 fb. The fiducial region definition for this cross section is based on the one described in table 2 with the following changes: the photon isolation and γ-centrality requirements were removed and the E_{T}^{γ} threshold was lowered to 15 GeV. This new, larger fiducial region includes the fiducial regions of both analyses used in the combination. The predicted cross section extrapolated to this fiducial region using VBFNLO is 9.6 ± 1.0 fb.

JHEP06(2023)082

9 Limits on anomalous quartic gauge couplings

The results presented in section 7 are used to set limits on anomalous QGCs via the VBS component of the measured electroweak process. New physics beyond the SM could induce anomalous QGCs, enhancing the $Z(\nu\bar{\nu})\gamma jj$ electroweak production cross section and modifying the kinematic distributions of the final-state bosons.

The effect of new physics introduced by aQGCs can be realised using an EFT [73] linearly parameterised by an effective Lagrangian as:

$$\mathcal{L} = \mathcal{L}^{\mathrm{SM}} + \sum_i \frac{c_i}{\Lambda^2}\mathcal{O}_i + \sum_j \frac{f_j}{\Lambda^4}\mathcal{O}_j,$$

where $\mathcal{O}_i$ and $\mathcal{O}_j$ are dimension-6 or dimension-8 operators induced by integrating out the new degrees of freedom, while c_i and f_j represent the numerical coefficients that are meant to be derivable from a more complete high-energy theory. The Λ term is a mass-dimension parameter associated with the energy scale of the new degrees of freedom that have been integrated out. The $Z(\nu\bar{\nu})\gamma jj$ VBS process is sensitive to anomalous quartic and triple gauge couplings. Since the latter are well constrained in diboson production [74], they are not explored in this paper. Among these higher-order operators, the dimension-8 ones are the lowest-dimensional operators inducing only quartic gauge-boson couplings without triple gauge-boson vertices. The impact of higher-dimensional operators is expected to be suppressed by more powers of the cut-off scale, Λ. However the linear terms in the EFT coefficient of the process amplitude originating from the operators of some dimensions higher than eight, can be suppressed by the same or smaller power of Λ, compared with the quadratic term originating from eight-dimensional operators. Therefore, it is assumed that such contributions are suppressed by the dimensionless coupling constant, f_j. Moreover, higher-dimensional terms are currently not available and are thus not taken into account.

Two categories of dimension-8 operators contribute to the couplings in the studied final state: $\mathcal{O}_{TX}$ ($X = 0$–9), constructed from the field-strength tensor; and $\mathcal{O}_{MX}$ ($X = 0$–7), constructed from both the Higgs $\mathrm{SU(2)_L}$ doublet derivatives and the field strength. Seven operators are considered in this study, and the corresponding (Wilson) coefficients are: f_{M0}/Λ^4, f_{M1}/Λ^4, f_{M2}/Λ^4, representing f_{MX} couplings, and f_{T0}/Λ^4, f_{T5}/Λ^4, f_{T8}/Λ^4 and f_{T9}/Λ^4, representing all types of f_{TX} couplings. The sensitivity of the $Z(\nu\bar{\nu})\gamma jj$ EWK final state to these operators is competitive with other electroweak production modes. The last two of these couplings are unique and can be probed only by the neutral quartic vertices.

A clipping technique is introduced to preserve unitarity at very high parton centre-of-mass energies. Advantage of this unitarity restoring technique among the other ones is simplicity of application and further theoretical interpretation of the limits. The anomalous signal contribution is set to zero for $m_{Z\gamma} > E_{\mathrm{c}}$ (using particle-level information), where E_{c} is a cut-off scale that is a free parameter. The chosen E_{c} value is based on the unitarity bounds for a given limit value calculated from partial-wave unitarity constraints [75].

Simulated $Z(\nu\bar{\nu})\gamma jj$ EWK events with non-zero EFT dimension-8 operator coefficients were generated by MadGraph5_aMC@NLO using decomposition of the process amplitude. For the case of only one non-zero Wilson coefficient at a time, the squared amplitude

JHEP06(2023)082

Coefficient	Observed limit [TeV^{-4}]	Expected limit [TeV^{-4}]
f_{T0}/Λ^4	$[-9.4, 8.4] \times 10^{-2}$	$[-1.3, 1.2] \times 10^{-1}$
f_{T5}/Λ^4	$[-8.8, 9.9] \times 10^{-2}$	$[-1.2, 1.3] \times 10^{-1}$
f_{T8}/Λ^4	$[-5.9, 5.9] \times 10^{-2}$	$[-8.1, 8.0] \times 10^{-2}$
f_{T9}/Λ^4	$[-1.3, 1.3] \times 10^{-1}$	$[-1.7, 1.7] \times 10^{-1}$
f_{M0}/Λ^4	$[-4.6, 4.6]$	$[-6.2, 6.2]$
f_{M1}/Λ^4	$[-7.7, 7.7]$	$[-1.0, 1.0] \times 10^{1}$
f_{M2}/Λ^4	$[-1.9, 1.9]$	$[-2.6, 2.6]$

Table 6. Observed and expected one-dimensional limits on dimension-8 aQGC coefficients. Limits are obtained by setting all aQGC coefficients except one to zero. Unitarity is not preserved.

is the following:

$$|A|^2 = |A_{\mathrm{SM}} + f_j A_j|^2 = |A_{\mathrm{SM}}|^2 + f_j 2\mathrm{Re}(A_{\mathrm{SM}} A_j^*) + {f_j}^2 |A_j|^2,$$

where $|A_{\mathrm{SM}} + f_j A_j|^2$ stands for the total amplitude squared with non-zero EFT parameter f_j, A_{SM} is the Standard Model amplitude, $f_j 2\mathrm{Re}(A_{\mathrm{SM}} A_j^*)$ is the amplitude of the interference between the SM and the EFT operator (the linear term of the process amplitude) and ${f_j}^2 |A_j|^2$ is the pure EFT operator contribution (quadratic term of the process amplitude). Individual samples using only one term at a time (SM, linear or quadratic terms) were generated for each operator. To obtain the events at a given value of the EFT coefficient, the respective sample is multiplied by the appropriate value (f_j or f_j^2).

Limits on the dimension-8 operator coefficients are calculated using test statistics based on the profile likelihood ratio. The likelihood function is constructed as a product of a Poisson distribution and a Gaussian constraint term with nuisance parameters representing the sources of systematic uncertainty. Data event and predicted yields for the limit-setting procedure are taken from the signal region with additional optimisation of the E_{T}^{γ} threshold using expected confidence intervals for the EFT coefficients. The sensitivity to the aQGC is the strongest at high E_{T}^{γ}, as it can be seen in figure 6. Therefore, the constraints on the aQGC parameters come from a bin, constructed from the SR by the optimisation of additional E_{T}^{γ} threshold and corrected for background normalisations from the background-only fit. Observed and expected 95% CL intervals for the EFT coefficients are presented for two cases: when the clipping technique is not applied, and hence unitarity is not preserved, and when it is applied, and hence unitarity is preserved. The results of the fit for the first and second cases are summarised in tables 6 and 7, respectively. The constraints are either competitive with or more stringent than those previously published by CMS [6, 9, 76].

Illustrations of the limits' dependence on E_{c} are given in figures 7 and 8. The regime in which E_{c} is less than 4 TeV is obtained with an E_{T}^{γ} threshold of 600 GeV (400 GeV) for f_{TX} (f_{MX}) couplings. The regime in which E_{c} exceeds 4 TeV is obtained with an E_{T}^{γ} threshold of 900 GeV. The E_{c} values for unitarised limits are obtained from the $E_{\mathrm{c}} < 4$ TeV regime by taking the point before the one where the limits' dependence crosses the unitarity bound. The infinity point in the figures indicates the limits obtained when the clipping technique is not applied, i.e. when $E_{\mathrm{c}} = \infty$. The E_{T}^{γ} thresholds are chosen so that the analysis reaches

JHEP06(2023)082

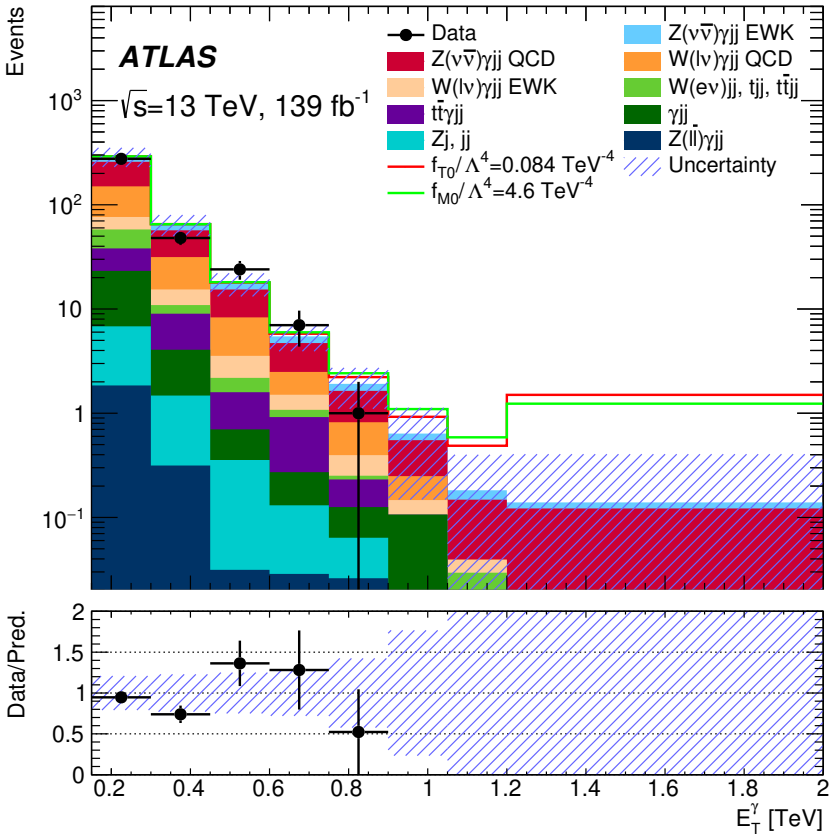

Figure 6. The E_{T}^{γ} distribution in the SR after the fit in the control regions. The red (green) line shows the expected number of events in the case of non-zero EFT coefficient f_{T0}/Λ^4 (f_{M0}/Λ^4) with the value shown in the legend. The vertical error bars on the data points correspond to the data statistical uncertainty. Overflows are included in the last bin. The lower panel shows the ratio of data to expected event yields. The uncertainty band corresponds to the combination of the MC statistical uncertainty and systematic uncertainties obtained in the fit.

Coefficient	E_{c} [TeV]	Observed limit [TeV^{-4}]	Expected limit [TeV^{-4}]
f_{T0}/Λ^4	1.7	$[-8.7, 7.1] \times 10^{-1}$	$[-8.9, 7.3] \times 10^{-1}$
f_{T5}/Λ^4	2.4	$[-3.4, 4.2] \times 10^{-1}$	$[-3.5, 4.3] \times 10^{-1}$
f_{T8}/Λ^4	1.7	$[-5.2, 5.2] \times 10^{-1}$	$[-5.3, 5.3] \times 10^{-1}$
f_{T9}/Λ^4	1.9	$[-7.9, 7.9] \times 10^{-1}$	$[-8.1, 8.1] \times 10^{-1}$
f_{M0}/Λ^4	0.7	$[-1.6, 1.6] \times 10^{2}$	$[-1.5, 1.5] \times 10^{2}$
f_{M1}/Λ^4	1.0	$[-1.6, 1.5] \times 10^{2}$	$[-1.4, 1.4] \times 10^{2}$
f_{M2}/Λ^4	1.0	$[-3.3, 3.2] \times 10^{1}$	$[-3.0, 3.0] \times 10^{1}$

Table 7. Observed and expected one-dimensional limits on dimension-8 aQGC coefficients in the region where unitarity is preserved. The cut-off scale E_{c} in the simulation is given for each parameter. Limits are obtained by setting all aQGC coefficients except one to zero.

JHEP06(2023)082

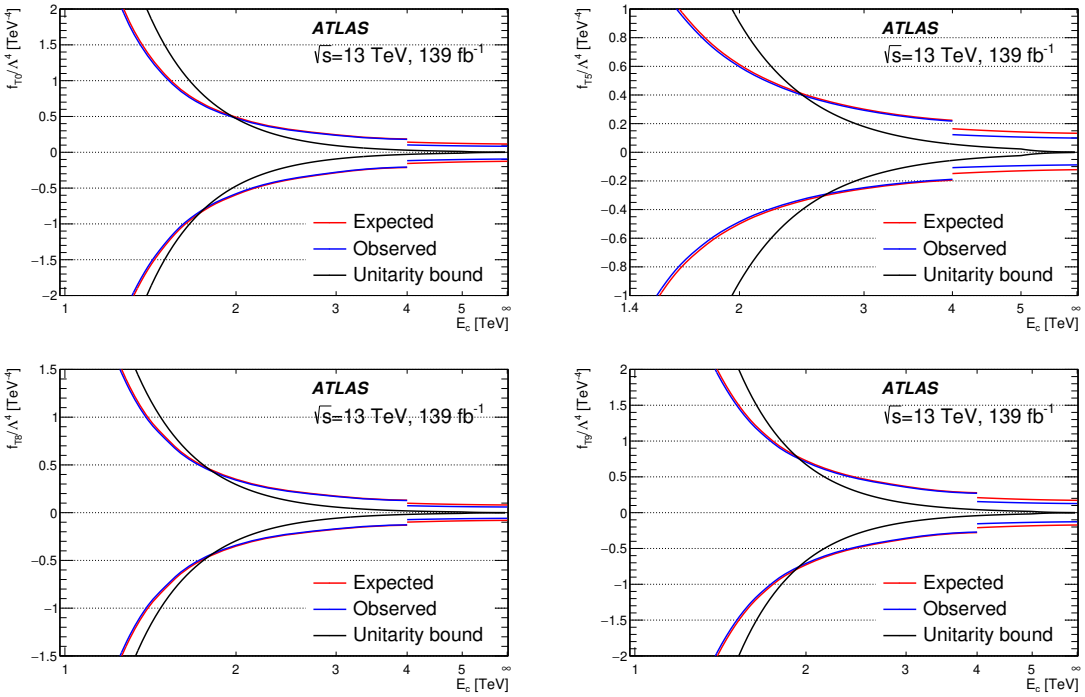

Figure 7. Evolution of the expected (red line) and observed (blue line) limits versus E_{c} values for f_{T0}/Λ^4, f_{T5}/Λ^4, f_{T8}/Λ^4 and f_{T9}/Λ^4. The unitarity bound is shown by the black line. The $E_{\mathrm{c}} < 4$ TeV regime was obtained with $E_{\mathrm{T}}^{\gamma} > 600$ GeV. The $E_{\mathrm{c}} > 4$ TeV regime was obtained with $E_{\mathrm{T}}^{\gamma} > 900$ GeV.

its highest sensitivity. They are different for the unitarised and non-unitarised cases, since the cut-off removes events with high E_{T}^{γ}.

10 Conclusion

A measurement of the fiducial cross section for electroweak production of $Z(\nu\bar{\nu})\gamma jj$ in the region of $E_{\mathrm{T}}^{\gamma} > 150\,\mathrm{GeV}$ is presented. Data from $\sqrt{s} = 13$ TeV pp collisions at the LHC were collected with the ATLAS detector during 2015–2018 and correspond to an integrated luminosity of 139 fb^{-1}. The dominant backgrounds come from QCD mediated $Z(\nu\bar{\nu})\gamma jj$ and $W\gamma jj$ processes and these are evaluated using a simultaneous fit to data. Other significant backgrounds from $e \to \gamma$ and $j \to \gamma$ misidentifications and $E_{\mathrm{T}}^{\mathrm{miss}}$ mismeasurement are evaluated using data-driven techniques. The measurement uses the invisible decay mode of the gauge boson, $Z \to \nu\bar{\nu}$, and is performed in a fiducial phase space closely matching the detector acceptance.

The observed (expected) signal significance is 3.2σ (3.7σ), which corresponds to evidence for this process in the given phase space used in the measurement. It was measured using a binned likelihood fit over the BDT classifier distribution. The measured cross section is $0.77^{+0.34}_{-0.30}$ fb, which is in agreement with SM predictions at NLO in perturbative

JHEP06(2023)082

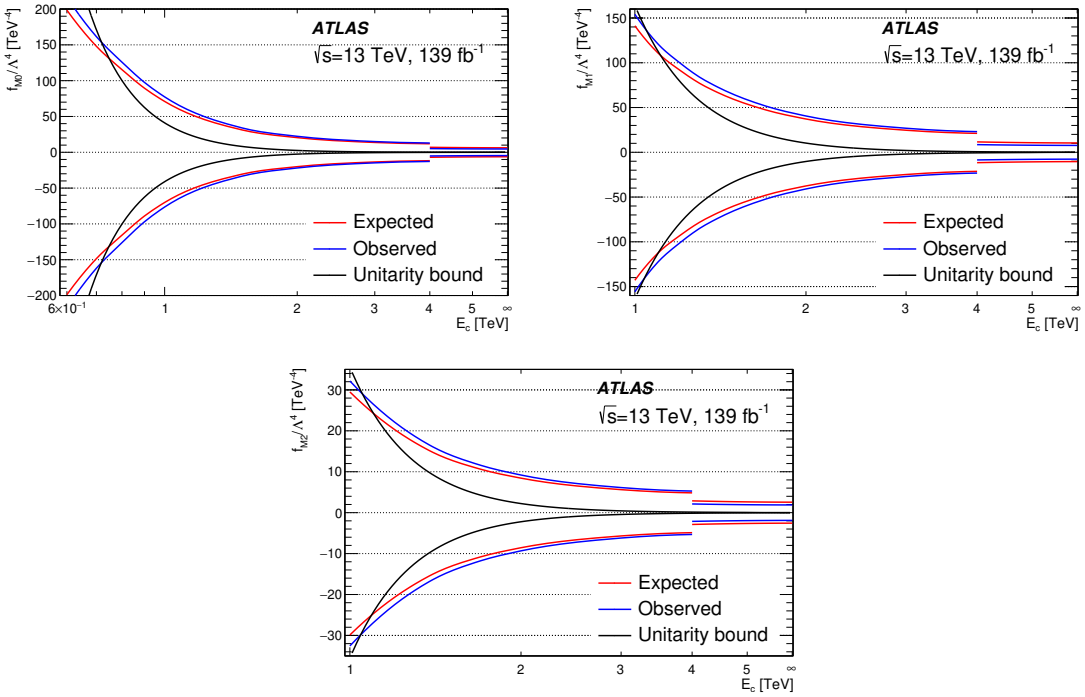

Figure 8. Evolution of the expected (red line) and observed (blue line) limits versus E_c values for f_{M0}/Λ^4, f_{M1}/Λ^4 and f_{M2}/Λ^4. The unitarity bound is shown by the black line. The $E_c < 4$ TeV regime was obtained with $E_T^\gamma > 400$ GeV. The $E_c > 4$ TeV regime was obtained with $E_T^\gamma > 900$ GeV.

QCD. The cross sections and kinematics are quoted for the sum of the three neutrino flavours.

The results of this study are combined with those of the previously published ATLAS observation of this process to increase the sensitivity. This gives an observed (expected) signal significance of 6.3σ (6.6σ).

Having found no significant deviations from SM predictions, the data are used to set limits on anomalous quartic gauge couplings. The limits are set on EFT dimension-8 operators f_{T0}/Λ^4, f_{T5}/Λ^4, f_{T8}/Λ^4, f_{T9}/Λ^4, f_{M0}/Λ^4, f_{M1}/Λ^4 and f_{M2}/Λ^4. These constraints are either competitive with or more stringent than those previously published by CMS. In particular, the constraints on the f_{T5}/Λ^4, f_{T8}/Λ^4 and f_{T9}/Λ^4 operators are significantly stronger than results previously published by ATLAS and CMS, based on either the full Run 2 dataset of 139 fb^{-1} or a partial dataset of 36 fb^{-1}.

Acknowledgments

We thank CERN for the very successful operation of the LHC, as well as the support staff from our institutions without whom ATLAS could not be operated efficiently.

We acknowledge the support of ANPCyT, Argentina; YerPhI, Armenia; ARC, Australia; BMWFW and FWF, Austria; ANAS, Azerbaijan; CNPq and FAPESP, Brazil; NSERC, NRC and CFI, Canada; CERN; ANID, Chile; CAS, MOST and NSFC, China;

JHEP06(2023)082

Minciencias, Colombia; MEYS CR, Czech Republic; DNRF and DNSRC, Denmark; IN2P3-CNRS and CEA-DRF/IRFU, France; SRNSFG, Georgia; BMBF, HGF and MPG, Germany; GSRI, Greece; RGC and Hong Kong SAR, China; ISF and Benoziyo Center, Israel; INFN, Italy; MEXT and JSPS, Japan; CNRST, Morocco; NWO, Netherlands; RCN, Norway; MEiN, Poland; FCT, Portugal; MNE/IFA, Romania; MESTD, Serbia; MSSR, Slovakia; ARRS and MIZŠ, Slovenia; DSI/NRF, South Africa; MICINN, Spain; SRC and Wallenberg Foundation, Sweden; SERI, SNSF and Cantons of Bern and Geneva, Switzerland; MOST, Taiwan; TENMAK, Türkiye; STFC, United Kingdom; DOE and NSF, United States of America. In addition, individual groups and members have received support from BCKDF, CANARIE, Compute Canada and CRC, Canada; PRIMUS 21/SCI/017 and UNCE SCI/013, Czech Republic; COST, ERC, ERDF, Horizon 2020 and Marie Skłodowska-Curie Actions, European Union; Investissements d'Avenir Labex, Investissements d'Avenir Idex and ANR, France; DFG and AvH Foundation, Germany; Herakleitos, Thales and Aristeia programmes co-financed by EU-ESF and the Greek NSRF, Greece; BSF-NSF and MINERVA, Israel; Norwegian Financial Mechanism 2014-2021, Norway; NCN and NAWA, Poland; La Caixa Banking Foundation, CERCA Programme Generalitat de Catalunya and PROMETEO and GenT Programmes Generalitat Valenciana, Spain; Göran Gustafssons Stiftelse, Sweden; The Royal Society and Leverhulme Trust, United Kingdom.

The crucial computing support from all WLCG partners is acknowledged gratefully, in particular from CERN, the ATLAS Tier-1 facilities at TRIUMF (Canada), NDGF (Denmark, Norway, Sweden), CC-IN2P3 (France), KIT/GridKA (Germany), INFN-CNAF (Italy), NL-T1 (Netherlands), PIC (Spain), ASGC (Taiwan), RAL (UK) and BNL (USA), the Tier-2 facilities worldwide and large non-WLCG resource providers. Major contributors of computing resources are listed in ref. [77].

Open Access. This article is distributed under the terms of the Creative Commons Attribution License (CC-BY 4.0), which permits any use, distribution and reproduction in any medium, provided the original author(s) and source are credited. SCOAP^3 supports the goals of the International Year of Basic Sciences for Sustainable Development.

References

[1] O.J.P. Eboli, M.C. Gonzalez-Garcia and S.M. Lietti, *Bosonic quartic couplings at CERN LHC*, *Phys. Rev. D* **69** (2004) 095005 [hep-ph/0310141] [INSPIRE].

[2] O.J.P. Éboli and M.C. Gonzalez-Garcia, *Classifying the bosonic quartic couplings*, *Phys. Rev. D* **93** (2016) 093013 [arXiv:1604.03555] [INSPIRE].

[3] M. Baak et al., *Working Group Report: Precision Study of Electroweak Interactions*, arXiv:1310.6708 [INSPIRE].

[4] E. Accomando, A. Ballestrero, A. Belhouari and E. Maina, *Isolating Vector Boson Scattering at the LHC: Gauge cancellations and the Equivalent Vector Boson Approximation vs. complete calculations*, *Phys. Rev. D* **74** (2006) 073010 [hep-ph/0608019] [INSPIRE].

[5] ATLAS collaboration, *The ATLAS Experiment at the CERN Large Hadron Collider*, 2008 *JINST* **3** S08003 [INSPIRE].

JHEP06(2023)082

[6] CMS collaboration, *Measurement of the electroweak production of $Z\gamma$ and two jets in proton-proton collisions at $\sqrt{s} = 13$ TeV and constraints on anomalous quartic gauge couplings*, *Phys. Rev. D* **104** (2021) 072001 [arXiv:2106.11082] [INSPIRE].

[7] ATLAS collaboration, *Observation of electroweak production of two jets in association with an isolated photon and missing transverse momentum, and search for a Higgs boson decaying into invisible particles at* 13 *TeV with the ATLAS detector*, *Eur. Phys. J. C* **82** (2022) 105 [arXiv:2109.00925] [INSPIRE].

[8] ATLAS collaboration, *Observation of electroweak production of two jets and a Z-boson pair*, *Nature Phys.* **19** (2023) 237 [arXiv:2004.10612] [INSPIRE].

[9] CMS collaboration, *Observation of electroweak production of $W\gamma$ with two jets in proton-proton collisions at $\sqrt{s} = 13$ TeV*, *Phys. Lett. B* **811** (2020) 135988 [arXiv:2008.10521] [INSPIRE].

[10] CMS collaboration, *Observation of electroweak production of same-sign W boson pairs in the two jet and two same-sign lepton final state in proton-proton collisions at $\sqrt{s} = 13$ TeV*, *Phys. Rev. Lett.* **120** (2018) 081801 [arXiv:1709.05822] [INSPIRE].

[11] ATLAS collaboration, *Observation of electroweak $W^{\pm}Z$ boson pair production in association with two jets in pp collisions at $\sqrt{s} = 13$ TeV with the ATLAS detector*, *Phys. Lett. B* **793** (2019) 469 [arXiv:1812.09740] [INSPIRE].

[12] ATLAS collaboration, *Observation of photon-induced W^+W^- production in pp collisions at $\sqrt{s} = 13$ TeV using the ATLAS detector*, *Phys. Lett. B* **816** (2021) 136190 [arXiv:2010.04019] [INSPIRE].

[13] ATLAS IBL collaboration, *Production and Integration of the ATLAS Insertable B-Layer*, 2018 *JINST* **13** T05008 [arXiv:1803.00844] [INSPIRE].

[14] ATLAS collaboration, *ATLAS Insertable B-Layer: Technical Design Report*, ATLAS-TDR-19 (2010).

[15] ATLAS collaboration, *Operation of the ATLAS trigger system in Run 2*, 2020 *JINST* **15** P10004 [arXiv:2007.12539] [INSPIRE].

[16] ATLAS collaboration, *The ATLAS Collaboration Software and Firmware*, ATL-SOFT-PUB-2021-001 (2021).

[17] ATLAS collaboration, *ATLAS data quality operations and performance for 2015–2018 data-taking*, 2020 *JINST* **15** P04003 [arXiv:1911.04632] [INSPIRE].

[18] ATLAS collaboration, *Luminosity determination in pp collisions at $\sqrt{s} = 13$ TeV using the ATLAS detector at the LHC*, ATLAS-CONF-2019-021 (2019).

[19] G. Avoni et al., *The new LUCID-2 detector for luminosity measurement and monitoring in ATLAS*, 2018 *JINST* **13** P07017 [INSPIRE].

[20] ATLAS collaboration, *The ATLAS Simulation Infrastructure*, *Eur. Phys. J. C* **70** (2010) 823 [arXiv:1005.4568] [INSPIRE].

[21] GEANT4 collaboration, *GEANT4 — a simulation toolkit*, *Nucl. Instrum. Meth. A* **506** (2003) 250 [INSPIRE].

[22] T. Sjöstrand, S. Mrenna and P.Z. Skands, *A Brief Introduction to PYTHIA 8.1*, *Comput. Phys. Commun.* **178** (2008) 852 [arXiv:0710.3820] [INSPIRE].

JHEP06(2023)082

[23] R.D. Ball et al., *Parton distributions with LHC data*, *Nucl. Phys. B* **867** (2013) 244 [arXiv:1207.1303] [INSPIRE].

[24] ATLAS collaboration, *The Pythia 8 A3 tune description of ATLAS minimum bias and inelastic measurements incorporating the Donnachie–Landshoff diffractive model*, ATL-PHYS-PUB-2016-017 (2016).

[25] T. Sjöstrand et al., *An introduction to PYTHIA 8.2*, *Comput. Phys. Commun.* **191** (2015) 159 [arXiv:1410.3012] [INSPIRE].

[26] D.J. Lange, *The EvtGen particle decay simulation package*, *Nucl. Instrum. Meth. A* **462** (2001) 152 [INSPIRE].

[27] K. Arnold et al., *VBFNLO: A Parton level Monte Carlo for processes with electroweak bosons*, *Comput. Phys. Commun.* **180** (2009) 1661 [arXiv:0811.4559] [INSPIRE].

[28] M. Bahr et al., *Herwig++ Physics and Manual*, *Eur. Phys. J. C* **58** (2008) 639 [arXiv:0803.0883] [INSPIRE].

[29] J. Bellm et al., *Herwig 7.0/Herwig++ 3.0 release note*, *Eur. Phys. J. C* **76** (2016) 196 [arXiv:1512.01178] [INSPIRE].

[30] SHERPA collaboration, *Event Generation with Sherpa 2.2*, *SciPost Phys.* **7** (2019) 034 [arXiv:1905.09127] [INSPIRE].

[31] T. Gleisberg and S. Höche, *Comix, a new matrix element generator*, *JHEP* **12** (2008) 039 [arXiv:0808.3674] [INSPIRE].

[32] S. Schumann and F. Krauss, *A Parton shower algorithm based on Catani-Seymour dipole factorisation*, *JHEP* **03** (2008) 038 [arXiv:0709.1027] [INSPIRE].

[33] S. Höche, F. Krauss, M. Schönherr and F. Siegert, *A critical appraisal of NLO+PS matching methods*, *JHEP* **09** (2012) 049 [arXiv:1111.1220] [INSPIRE].

[34] S. Höche, F. Krauss, M. Schönherr and F. Siegert, *QCD matrix elements + parton showers: The NLO case*, *JHEP* **04** (2013) 027 [arXiv:1207.5030] [INSPIRE].

[35] S. Catani, F. Krauss, R. Kuhn and B.R. Webber, *QCD matrix elements + parton showers*, *JHEP* **11** (2001) 063 [hep-ph/0109231] [INSPIRE].

[36] S. Höche, F. Krauss, S. Schumann and F. Siegert, *QCD matrix elements and truncated showers*, *JHEP* **05** (2009) 053 [arXiv:0903.1219] [INSPIRE].

[37] OPENLOOPS 2 collaboration, *OpenLoops 2*, *Eur. Phys. J. C* **79** (2019) 866 [arXiv:1907.13071] [INSPIRE].

[38] F. Cascioli, P. Maierhofer and S. Pozzorini, *Scattering Amplitudes with Open Loops*, *Phys. Rev. Lett.* **108** (2012) 111601 [arXiv:1111.5206] [INSPIRE].

[39] A. Denner, S. Dittmaier and L. Hofer, *Collier: a Fortran-based Complex One-Loop Library In Extended Regularizations*, *Comput. Phys. Commun.* **212** (2017) 220 [arXiv:1604.06792] [INSPIRE].

[40] NNPDF collaboration, *Parton distributions for the LHC Run II*, *JHEP* **04** (2015) 040 [arXiv:1410.8849] [INSPIRE].

[41] C. Anastasiou, L.J. Dixon, K. Melnikov and F. Petriello, *High precision QCD at hadron colliders: Electroweak gauge boson rapidity distributions at NNLO*, *Phys. Rev. D* **69** (2004) 094008 [hep-ph/0312266] [INSPIRE].

JHEP06(2023)082

[42] J. Alwall et al., *The automated computation of tree-level and next-to-leading order differential cross sections, and their matching to parton shower simulations*, *JHEP* **07** (2014) 079 [arXiv:1405.0301] [INSPIRE].

[43] R. Frederix and S. Frixione, *Merging meets matching in MC@NLO*, *JHEP* **12** (2012) 061 [arXiv:1209.6215] [INSPIRE].

[44] P. Nason, *A New method for combining NLO QCD with shower Monte Carlo algorithms*, *JHEP* **11** (2004) 040 [hep-ph/0409146] [INSPIRE].

[45] S. Frixione, P. Nason and C. Oleari, *Matching NLO QCD computations with Parton Shower simulations: the POWHEG method*, *JHEP* **11** (2007) 070 [arXiv:0709.2092] [INSPIRE].

[46] S. Alioli, P. Nason, C. Oleari and E. Re, *NLO single-top production matched with shower in POWHEG: s- and t-channel contributions*, *JHEP* **09** (2009) 111 [*Erratum ibid.* **02** (2010) 011] [arXiv:0907.4076] [INSPIRE].

[47] S. Alioli, P. Nason, C. Oleari and E. Re, *A general framework for implementing NLO calculations in shower Monte Carlo programs: the POWHEG BOX*, *JHEP* **06** (2010) 043 [arXiv:1002.2581] [INSPIRE].

[48] J. Alwall et al., *MadGraph 5: Going Beyond*, *JHEP* **06** (2011) 128 [arXiv:1106.0522] [INSPIRE].

[49] ATLAS collaboration, *ATLAS Pythia 8 tunes to 7 TeV data*, ATL-PHYS-PUB-2014-021 (2014).

[50] H.-L. Lai et al., *New parton distributions for collider physics*, *Phys. Rev. D* **82** (2010) 074024 [arXiv:1007.2241] [INSPIRE].

[51] ATLAS collaboration, *Measurement of the photon identification efficiencies with the ATLAS detector using LHC Run 2 data collected in 2015 and 2016*, *Eur. Phys. J. C* **79** (2019) 205 [arXiv:1810.05087] [INSPIRE].

[52] ATLAS collaboration, *Performance of electron and photon triggers in ATLAS during LHC Run 2*, *Eur. Phys. J. C* **80** (2020) 47 [arXiv:1909.00761] [INSPIRE].

[53] ATLAS collaboration, *Electron and photon performance measurements with the ATLAS detector using the 2015–2017 LHC proton-proton collision data*, 2019 *JINST* **14** P12006 [arXiv:1908.00005] [INSPIRE].

[54] ATLAS collaboration, *Muon reconstruction and identification efficiency in ATLAS using the full Run 2 pp collision data set at* $\sqrt{s} = 13$ *TeV*, *Eur. Phys. J. C* **81** (2021) 578 [arXiv:2012.00578] [INSPIRE].

[55] ATLAS collaboration, *Characterisation and mitigation of beam-induced backgrounds observed in the ATLAS detector during the 2011 proton-proton run*, 2013 *JINST* **8** P07004 [arXiv:1303.0223] [INSPIRE].

[56] M. Cacciari, G.P. Salam and G. Soyez, *The anti-k_t jet clustering algorithm*, *JHEP* **04** (2008) 063 [arXiv:0802.1189] [INSPIRE].

[57] M. Cacciari, G.P. Salam and G. Soyez, *FastJet User Manual*, *Eur. Phys. J. C* **72** (2012) 1896 [arXiv:1111.6097] [INSPIRE].

[58] ATLAS collaboration, *Jet energy scale measurements and their systematic uncertainties in proton-proton collisions at* $\sqrt{s} = 13$ *TeV with the ATLAS detector*, *Phys. Rev. D* **96** (2017) 072002 [arXiv:1703.09665] [INSPIRE].

JHEP06(2023)082

[59] ATLAS collaboration, *Jet Calibration and Systematic Uncertainties for Jets Reconstructed in the ATLAS Detector at* $\sqrt{s} = 13$ *TeV*, ATL-PHYS-PUB-2015-015 (2015).

[60] ATLAS collaboration, *Performance of pile-up mitigation techniques for jets in pp collisions at* $\sqrt{s} = 8$ *TeV using the ATLAS detector*, *Eur. Phys. J. C* **76** (2016) 581 [arXiv:1510.03823] [INSPIRE].

[61] ATLAS collaboration, *Identification and rejection of pile-up jets at high pseudorapidity with the ATLAS detector*, *Eur. Phys. J. C* **77** (2017) 580 [*Erratum ibid.* **77** (2017) 712] [arXiv:1705.02211] [INSPIRE].

[62] ATLAS collaboration, *Performance of missing transverse momentum reconstruction with the ATLAS detector using proton-proton collisions at* $\sqrt{s} = 13$ *TeV*, *Eur. Phys. J. C* **78** (2018) 903 [arXiv:1802.08168] [INSPIRE].

[63] ATLAS collaboration, *Object-based missing transverse momentum significance in the ATLAS Detector*, ATLAS-CONF-2018-038 (2018).

[64] ATLAS collaboration, *Measurement of Wgamma and Zgamma production in proton-proton collisions at* $\sqrt{s} = 7$ *TeV with the ATLAS Detector*, *JHEP* **09** (2011) 072 [arXiv:1106.1592] [INSPIRE].

[65] ATLAS collaboration, *Measurements of inclusive and differential cross-sections of combined* $t\bar{t}\gamma$ *and* $tW\gamma$ *production in the* $e\mu$ *channel at 13 TeV with the ATLAS detector*, *JHEP* **09** (2020) 049 [arXiv:2007.06946] [INSPIRE].

[66] ATLAS collaboration, *A new tool for measuring detector performance in ATLAS*, *J. Phys. Conf. Ser.* **219** (2010) 032023 [INSPIRE].

[67] ATLAS collaboration, *Measurement of the inclusive isolated prompt photon cross section in pp collisions at* $\sqrt{s} = 7$ *TeV with the ATLAS detector*, *Phys. Rev. D* **83** (2011) 052005 [arXiv:1012.4389] [INSPIRE].

[68] ATLAS collaboration, *Measurement of the photon identification efficiencies with the ATLAS detector using LHC Run-1 data*, *Eur. Phys. J. C* **76** (2016) 666 [arXiv:1606.01813] [INSPIRE].

[69] J. Butterworth et al., *PDF4LHC recommendations for LHC Run II*, *J. Phys. G* **43** (2016) 023001 [arXiv:1510.03865] [INSPIRE].

[70] A. Höcker et al., *TMVA - Toolkit for Multivariate Data Analysis*, physics/0703039.

[71] K. Cranmer, G. Lewis, L. Moneta, A. Shibata and W. Verkerke, *HistFactory: A tool for creating statistical models for use with RooFit and RooStats*, CERN-OPEN-2012-016, (2012).

[72] G. Cowan, K. Cranmer, E. Gross and O. Vitells, *Asymptotic formulae for likelihood-based tests of new physics*, *Eur. Phys. J. C* **71** (2011) 1554 [*Erratum ibid.* **73** (2013) 2501] [arXiv:1007.1727] [INSPIRE].

[73] C. Degrande et al., *Effective Field Theory: A Modern Approach to Anomalous Couplings*, *Annals Phys.* **335** (2013) 21 [arXiv:1205.4231] [INSPIRE].

[74] ATLAS collaboration, *Measurement of the* $Z\gamma \to \nu\bar{\nu}\gamma$ *production cross section in pp collisions at* $\sqrt{s} = 13$ *TeV with the ATLAS detector and limits on anomalous triple gauge-boson couplings*, *JHEP* **12** (2018) 010 [arXiv:1810.04995] [INSPIRE].

[75] E.d.S. Almeida, O.J.P. Éboli and M.C. Gonzalez–Garcia, *Unitarity constraints on anomalous quartic couplings*, *Phys. Rev. D* **101** (2020) 113003 [arXiv:2004.05174] [INSPIRE].

JHEP06(2023)082

[76] CMS collaboration, *Search for anomalous electroweak production of vector boson pairs in association with two jets in proton-proton collisions at 13 TeV*, *Phys. Lett. B* **798** (2019) 134985 [arXiv:1905.07445] [INSPIRE].

[77] ATLAS collaboration, *ATLAS Computing Acknowledgements* ATL-SOFT-PUB-2021-003, CERN, Geneva (2021).

JHEP06(2023)082

The ATLAS collaboration

G. Aad[101], B. Abbott[119], D.C. Abbott[102], K. Abeling[55], S.H. Abidi[29], A. Aboulhorma[35e], H. Abramowicz[150], H. Abreu[149], Y. Abulaiti[116], A.C. Abusleme Hoffman[136a], B.S. Acharya[68a,68b,o], B. Achkar[55], C. Adam Bourdarios[4], L. Adamczyk[84a], L. Adamek[154], S.V. Addepalli[26], J. Adelman[114], A. Adiguzel[21c], S. Adorni[56], T. Adye[133], A.A. Affolder[135], Y. Afik[36], M.N. Agaras[13], J. Agarwala[72a,72b], A. Aggarwal[99], C. Agheorghiesei[27c], J.A. Aguilar-Saavedra[129f], A. Ahmad[36], F. Ahmadov[38,w], W.S. Ahmed[103], S. Ahuja[94], X. Ai[48], G. Aielli[75a,75b], I. Aizenberg[167], M. Akbiyik[99], T.P.A. Åkesson[97], A.V. Akimov[37], K. Al Khoury[41], G.L. Alberghi[23b], J. Albert[163], P. Albicocco[53], M.J. Alconada Verzini[89], S. Alderweireldt[52], M. Aleksa[36], I.N. Aleksandrov[38], C. Alexa[27b], T. Alexopoulos[10], A. Alfonsi[113], F. Alfonsi[23b], M. Alhroob[119], B. Ali[131], S. Ali[147], M. Aliev[37], G. Alimonti[70a], W. Alkakhi[55], C. Allaire[36], B.M.M. Allbrooke[145], P.P. Allport[20], A. Aloisio[71a,71b], F. Alonso[89], C. Alpigiani[137], E. Alunno Camelia[75a,75b], M. Alvarez Estevez[98], M.G. Alviggi[71a,71b], Y. Amaral Coutinho[81b], A. Ambler[103], C. Amelung[36], C.G. Ames[108], D. Amidei[105], S.P. Amor Dos Santos[129a], S. Amoroso[48], K.R. Amos[161], C.S. Amrouche[56], V. Ananiev[124], C. Anastopoulos[138], T. Andeen[11], J.K. Anders[19], S.Y. Andrean[47a,47b], A. Andreazza[70a,70b], S. Angelidakis[9], A. Angerami[41,y], A.V. Anisenkov[37], A. Annovi[73a], C. Antel[56], M.T. Anthony[138], E. Antipov[120], M. Antonelli[53], D.J.A. Antrim[17a], F. Anulli[74a], M. Aoki[82], T. Aoki[152], J.A. Aparisi Pozo[161], M.A. Aparo[145], L. Aperio Bella[48], C. Appelt[18], N. Aranzabal[36], V. Araujo Ferraz[81a], C. Arcangeletti[53], A.T.H. Arce[51], E. Arena[91], J-F. Arguin[107], S. Argyropoulos[54], J.-H. Arling[48], A.J. Armbruster[36], O. Arnaez[154], H. Arnold[113], Z.P. Arrubarrena Tame[108], G. Artoni[74a,74b], H. Asada[110], K. Asai[117], S. Asai[152], N.A. Asbah[61], J. Assahsah[35d], K. Assamagan[29], R. Astalos[28a], R.J. Atkin[33a], M. Atkinson[160], N.B. Atlay[18], H. Atmani[62b], P.A. Atmasiddha[105], K. Augsten[131], S. Auricchio[71a,71b], A.D. Auriol[20], V.A. Austrup[169], G. Avner[149], G. Avolio[36], K. Axiotis[56], M.K. Ayoub[14c], G. Azuelos[107,aa], D. Babal[28a], H. Bachacou[134], K. Bachas[151,q], A. Bachiu[34], F. Backman[47a,47b], A. Badea[61], P. Bagnaia[74a,74b], M. Bahmani[18], A.J. Bailey[161], V.R. Bailey[160], J.T. Baines[133], C. Bakalis[10], O.K. Baker[170], P.J. Bakker[113], E. Bakos[15], D. Bakshi Gupta[8], S. Balaji[146], R. Balasubramanian[113], E.M. Baldin[37], P. Balek[132], E. Ballabene[70a,70b], F. Balli[134], L.M. Baltes[63a], W.K. Balunas[32], J. Balz[99], E. Banas[85], M. Bandieramonte[128], A. Bandyopadhyay[24], S. Bansal[24], L. Barak[150], E.L. Barberio[104], D. Barberis[57b,57a], M. Barbero[101], G. Barbour[95], K.N. Barends[33a], T. Barillari[109], M-S. Barisits[36], T. Barklow[142], R.M. Barnett[17a], P. Baron[121], D.A. Baron Moreno[100], A. Baroncelli[62a], G. Barone[29], A.J. Barr[125], L. Barranco Navarro[47a,47b], F. Barreiro[98], J. Barreiro Guimarães da Costa[14a], U. Barron[150], M.G. Barros Teixeira[129a], S. Barsov[37], F. Bartels[63a], R. Bartoldus[142], A.E. Barton[90], P. Bartos[28a], A. Basalaev[48], A. Basan[99], M. Baselga[49], I. Bashta[76a,76b], A. Bassalat[66,ag], M.J. Basso[154], C.R. Basson[100], R.L. Bates[59], S. Batlamous[35e], J.R. Batley[32], B. Batool[140], M. Battaglia[135], D. Battulga[18], M. Bauce[74a,74b], P. Bauer[24], A. Bayirli[21a],

JHEP06(2023)082

J.B. Beacham[51], T. Beau[126], P.H. Beauchemin[157], F. Becherer[54], P. Bechtle[24], H.P. Beck[19,p], K. Becker[165], C. Becot[48], A.J. Beddall[21d], V.A. Bednyakov[38], C.P. Bee[144], L.J. Beemster[15], T.A. Beermann[36], M. Begalli[81d,81d], M. Begel[29], A. Behera[144], J.K. Behr[48], C. Beirao Da Cruz E Silva[36], J.F. Beirer[55,36], F. Beisiegel[24], M. Belfkir[115b], G. Bella[150], L. Bellagamba[23b], A. Bellerive[34], P. Bellos[20], K. Beloborodov[37], K. Belotskiy[37], N.L. Belyaev[37], D. Benchekroun[35a], F. Bendebba[35a], Y. Benhammou[150], D.P. Benjamin[29], M. Benoit[29], J.R. Bensinger[26], S. Bentvelsen[113], L. Beresford[36], M. Beretta[53], D. Berge[18], E. Bergeaas Kuutmann[159], N. Berger[4], B. Bergmann[131], J. Beringer[17a], S. Berlendis[7], G. Bernardi[5], C. Bernius[142], F.U. Bernlochner[24], T. Berry[94], P. Berta[132], A. Berthold[50], I.A. Bertram[90], S. Bethke[109], A. Betti[74a,74b], A.J. Bevan[93], M. Bhamjee[33c], S. Bhatta[144], D.S. Bhattacharya[164], P. Bhattarai[26], V.S. Bhopatkar[120], R. Bi[29,ad], R.M. Bianchi[128], O. Biebel[108], R. Bielski[122], M. Biglietti[76a], T.R.V. Billoud[131], M. Bindi[55], A. Bingul[21b], C. Bini[74a,74b], S. Biondi[23b,23a], A. Biondini[91], C.J. Birch-sykes[100], G.A. Bird[20,133], M. Birman[167], T. Bisanz[36], E. Bisceglie[43b,43a], D. Biswas[168,k], A. Bitadze[100], K. Bjørke[124], I. Bloch[48], C. Blocker[26], A. Blue[59], U. Blumenschein[93], J. Blumenthal[99], G.J. Bobbink[113], V.S. Bobrovnikov[37], M. Boehler[54], D. Bogavac[36], A.G. Bogdanchikov[37], C. Bohm[47a], V. Boisvert[94], P. Bokan[48], T. Bold[84a], M. Bomben[5], M. Bona[93], M. Boonekamp[134], C.D. Booth[94], A.G. Borbély[59], H.M. Borecka-Bielska[107], L.S. Borgna[95], G. Borissov[90], D. Bortoletto[125], D. Boscherini[23b], M. Bosman[13], J.D. Bossio Sola[36], K. Bouaouda[35a], J. Boudreau[128], E.V. Bouhova-Thacker[90], D. Boumediene[40], R. Bouquet[5], A. Boveia[118], J. Boyd[36], D. Boye[29], I.R. Boyko[38], J. Bracinik[20], N. Brahimi[62d], G. Brandt[169], O. Brandt[32], F. Braren[48], B. Brau[102], J.E. Brau[122], K. Brendlinger[48], R. Brener[167], L. Brenner[36], R. Brenner[159], S. Bressler[167], B. Brickwedde[99], D. Britton[59], D. Britzger[109], I. Brock[24], G. Brooijmans[41], W.K. Brooks[136f], E. Brost[29], P.A. Bruckman de Renstrom[85], B. Brüers[48], D. Bruncko[28b,*], A. Bruni[23b], G. Bruni[23b], M. Bruschi[23b], N. Bruscino[74a,74b], L. Bryngemark[142], T. Buanes[16], Q. Buat[137], P. Buchholz[140], A.G. Buckley[59], I.A. Budagov[38,*], M.K. Bugge[124], O. Bulekov[37], B.A. Bullard[61], S. Burdin[91], C.D. Burgard[48], A.M. Burger[40], B. Burghgrave[8], J.T.P. Burr[32], C.D. Burton[11], J.C. Burzynski[141], E.L. Busch[41], V. Büscher[99], P.J. Bussey[59], J.M. Butler[25], C.M. Buttar[59], J.M. Butterworth[95], W. Buttinger[133], C.J. Buxo Vazquez[106], A.R. Buzykaev[37], G. Cabras[23b], S. Cabrera Urbán[161], D. Caforio[58], H. Cai[128], Y. Cai[14a,14d], V.M.M. Cairo[36], O. Cakir[3a], N. Calace[36], P. Calafiura[17a], G. Calderini[126], P. Calfayan[67], G. Callea[59], L.P. Caloba[81b], D. Calvet[40], S. Calvet[40], T.P. Calvet[101], M. Calvetti[73a,73b], R. Camacho Toro[126], S. Camarda[36], D. Camarero Munoz[26], P. Camarri[75a,75b], M.T. Camerlingo[76a,76b], D. Cameron[124], C. Camincher[163], M. Campanelli[95], A. Camplani[42], V. Canale[71a,71b], A. Canesse[103], M. Cano Bret[79], J. Cantero[161], Y. Cao[160], F. Capocasa[26], M. Capua[43b,43a], A. Carbone[70a,70b], R. Cardarelli[75a], J.C.J. Cardenas[8], F. Cardillo[161], T. Carli[36], G. Carlino[71a], B.T. Carlson[128,r], E.M. Carlson[163,155a], L. Carminati[70a,70b], M. Carnesale[74a,74b], S. Caron[112], E. Carquin[136f], S. Carrá[70a,70b], G. Carratta[23b,23a], F. Carrio Argos[33g], J.W.S. Carter[154], T.M. Carter[52], M.P. Casado[13,h], A.F. Casha[154],

JHEP06(2023)082

E.G. Castiglia[170], F.L. Castillo[63a], L. Castillo Garcia[13], V. Castillo Gimenez[161], N.F. Castro[129a,129e], A. Catinaccio[36], J.R. Catmore[124], V. Cavaliere[29], N. Cavalli[23b,23a], V. Cavasinni[73a,73b], E. Celebi[21a], F. Celli[125], M.S. Centonze[69a,69b], K. Cerny[121], A.S. Cerqueira[81a], A. Cerri[145], L. Cerrito[75a,75b], F. Cerutti[17a], A. Cervelli[23b], S.A. Cetin[21d], Z. Chadi[35a], D. Chakraborty[114], M. Chala[129f], J. Chan[168], W.Y. Chan[152], J.D. Chapman[32], B. Chargeishvili[148b], D.G. Charlton[20], T.P. Charman[93], M. Chatterjee[19], S. Chekanov[6], S.V. Chekulaev[155a], G.A. Chelkov[38,a], A. Chen[105], B. Chen[150], B. Chen[163], C. Chen[62a], H. Chen[14c], H. Chen[29], J. Chen[62c], J. Chen[26], S. Chen[152], S.J. Chen[14c], X. Chen[62c], X. Chen[14b,z], Y. Chen[62a], C.L. Cheng[168], H.C. Cheng[64a], A. Cheplakov[38], E. Cheremushkina[48], E. Cherepanova[113], R. Cherkaoui El Moursli[35e], E. Cheu[7], K. Cheung[65], L. Chevalier[134], V. Chiarella[53], G. Chiarelli[73a], N. Chiedde[101], G. Chiodini[69a], A.S. Chisholm[20], A. Chitan[27b], M. Chitishvili[161], Y.H. Chiu[163], M.V. Chizhov[38], K. Choi[11], A.R. Chomont[74a,74b], Y. Chou[102], E.Y.S. Chow[113], T. Chowdhury[33g], L.D. Christopher[33g], K.L. Chu[64a], M.C. Chu[64a], X. Chu[14a,14d], J. Chudoba[130], J.J. Chwastowski[85], D. Cieri[109], K.M. Ciesla[84a], V. Cindro[92], A. Ciocio[17a], F. Cirotto[71a,71b], Z.H. Citron[167,l], M. Citterio[70a], D.A. Ciubotaru[27b], B.M. Ciungu[154], A. Clark[56], P.J. Clark[52], J.M. Clavijo Columbie[48], S.E. Clawson[100], C. Clement[47a,47b], J. Clercx[48], L. Clissa[23b,23a], Y. Coadou[101], M. Cobal[68a,68c], A. Coccaro[57b], R.F. Coelho Barrue[129a], R. Coelho Lopes De Sa[102], S. Coelli[70a], H. Cohen[150], A.E.C. Coimbra[70a,70b], B. Cole[41], J. Collot[60], P. Conde Muiño[129a,129g], M.P. Connell[33c], S.H. Connell[33c], I.A. Connelly[59], E.I. Conroy[125], F. Conventi[71a,ab], H.G. Cooke[20], A.M. Cooper-Sarkar[125], F. Cormier[162], L.D. Corpe[36], M. Corradi[74a,74b], E.E. Corrigan[97], F. Corriveau[103,v], A. Cortes-Gonzalez[18], M.J. Costa[161], F. Costanza[4], D. Costanzo[138], B.M. Cote[118], G. Cowan[94], J.W. Cowley[32], K. Cranmer[116], S. Crépé-Renaudin[60], F. Crescioli[126], M. Cristinziani[140], M. Cristoforetti[77a,77b,c], V. Croft[157], G. Crosetti[43b,43a], A. Cueto[36], T. Cuhadar Donszelmann[158], H. Cui[14a,14d], Z. Cui[7], A.R. Cukierman[142], W.R. Cunningham[59], F. Curcio[43b,43a], P. Czodrowski[36], M.M. Czurylo[63b], M.J. Da Cunha Sargedas De Sousa[62a], J.V. Da Fonseca Pinto[81b], C. Da Via[100], W. Dabrowski[84a], T. Dado[49], S. Dahbi[33g], T. Dai[105], C. Dallapiccola[102], M. Dam[42], G. D'amen[29], V. D'Amico[108], J. Damp[99], J.R. Dandoy[127], M.F. Daneri[30], M. Danninger[141], V. Dao[36], G. Darbo[57b], S. Darmora[6], S.J. Das[29], S. D'Auria[70a,70b], C. David[155b], T. Davidek[132], D.R. Davis[51], B. Davis-Purcell[34], I. Dawson[93], K. De[8], R. De Asmundis[71a], M. De Beurs[113], N. De Biase[48], S. De Castro[23b,23a], N. De Groot[112], P. de Jong[113], H. De la Torre[106], A. De Maria[14c], A. De Salvo[74a], U. De Sanctis[75a,75b], A. De Santo[145], J.B. De Vivie De Regie[60], D.V. Dedovich[38], J. Degens[113], A.M. Deiana[44], F. Del Corso[23b,23a], J. Del Peso[98], F. Del Rio[63a], F. Deliot[134], C.M. Delitzsch[49], M. Della Pietra[71a,71b], D. Della Volpe[56], A. Dell'Acqua[36], L. Dell'Asta[70a,70b], M. Delmastro[4], P.A. Delsart[60], S. Demers[170], M. Demichev[38], S.P. Denisov[37], L. D'Eramo[114], D. Derendarz[85], F. Derue[126], P. Dervan[91], K. Desch[24], K. Dette[154], C. Deutsch[24], P.O. Deviveiros[36], F.A. Di Bello[74a,74b], A. Di Ciaccio[75a,75b], L. Di Ciaccio[4], A. Di Domenico[74a,74b], C. Di Donato[71a,71b], A. Di Girolamo[36],

JHEP06(2023)082

G. Di Gregorio[73a,73b], A. Di Luca[77a,77b], B. Di Micco[76a,76b], R. Di Nardo[76a,76b], C. Diaconu[101], F.A. Dias[113], T. Dias Do Vale[141], M.A. Diaz[136a,136b], F.G. Diaz Capriles[24], M. Didenko[161], E.B. Diehl[105], L. Diehl[54], S. Díez Cornell[48], C. Diez Pardos[140], C. Dimitriadi[24,159], A. Dimitrievska[17a], W. Ding[14b], J. Dingfelder[24], I-M. Dinu[27b], S.J. Dittmeier[63b], F. Dittus[36], F. Djama[101], T. Djobava[148b], J.I. Djuvsland[16], C. Doglioni[100,97], J. Dolejsi[132], Z. Dolezal[132], M. Donadelli[81c], B. Dong[62c], J. Donini[40], A. D'Onofrio[14c], M. D'Onofrio[91], J. Dopke[133], A. Doria[71a], M.T. Dova[89], A.T. Doyle[59], M.A. Draguet[125], E. Drechsler[141], E. Dreyer[167], I. Drivas-koulouris[10], A.S. Drobac[157], D. Du[62a], T.A. du Pree[113], F. Dubinin[37], M. Dubovsky[28a], E. Duchovni[167], G. Duckeck[108], O.A. Ducu[27b], D. Duda[109], A. Dudarev[36], M. D'uffizi[100], L. Duflot[66], M. Dührssen[36], C. Dülsen[169], A.E. Dumitriu[27b], M. Dunford[63a], S. Dungs[49], K. Dunne[47a,47b], A. Duperrin[101], H. Duran Yildiz[3a], M. Düren[58], A. Durglishvili[148b], B.L. Dwyer[114], G.I. Dyckes[17a], M. Dyndal[84a], S. Dysch[100], B.S. Dziedzic[85], Z.O. Earnshaw[145], B. Eckerova[28a], M.G. Eggleston[51], E. Egidio Purcino De Souza[81b], L.F. Ehrke[56], G. Eigen[16], K. Einsweiler[17a], T. Ekelof[159], P.A. Ekman[97], Y. El Ghazali[35b], H. El Jarrari[35e,147], A. El Moussaouy[35a], V. Ellajosyula[159], M. Ellert[159], F. Ellinghaus[169], A.A. Elliot[93], N. Ellis[36], J. Elmsheuser[29], M. Elsing[36], D. Emeliyanov[133], A. Emerman[41], Y. Enari[152], I. Ene[17a], S. Epari[13], J. Erdmann[49], A. Ereditato[19], P.A. Erland[85], M. Errenst[169], M. Escalier[66], C. Escobar[161], E. Etzion[150], G. Evans[129a], H. Evans[67], M.O. Evans[145], A. Ezhilov[37], S. Ezzarqtouni[35a], F. Fabbri[59], L. Fabbri[23b,23a], G. Facini[95], V. Fadeyev[135], R.M. Fakhrutdinov[37], S. Falciano[74a], P.J. Falke[24], S. Falke[36], J. Faltova[132], Y. Fan[14a], Y. Fang[14a,14d], G. Fanourakis[46], M. Fanti[70a,70b], M. Faraj[68a,68b], A. Farbin[8], A. Farilla[76a], T. Farooque[106], S.M. Farrington[52], F. Fassi[35e], D. Fassouliotis[9], M. Faucci Giannelli[75a,75b], W.J. Fawcett[32], L. Fayard[66], P. Federicova[130], O.L. Fedin[37,a], G. Fedotov[37], M. Feickert[160], L. Feligioni[101], A. Fell[138], D.E. Fellers[122], C. Feng[62b], M. Feng[14b], Z. Feng[113], M.J. Fenton[158], A.B. Fenyuk[37], L. Ferencz[48], S.W. Ferguson[45], J. Pretel[54], J. Ferrando[48], A. Ferrari[159], P. Ferrari[113], R. Ferrari[72a], D. Ferrere[56], C. Ferretti[105], F. Fiedler[99], A. Filipčič[92], E.K. Filmer[1], F. Filthaut[112], M.C.N. Fiolhais[129a,129c,b], L. Fiorini[161], F. Fischer[140], W.C. Fisher[106], T. Fitschen[20], I. Fleck[140], P. Fleischmann[105], T. Flick[169], L. Flores[127], M. Flores[33d], L.R. Flores Castillo[64a], F.M. Follega[77a,77b], N. Fomin[16], J.H. Foo[154], B.C. Forland[67], A. Formica[134], A.C. Forti[100], E. Fortin[101], A.W. Fortman[61], M.G. Foti[17a], L. Fountas[9], D. Fournier[66], H. Fox[90], P. Francavilla[73a,73b], S. Francescato[61], M. Franchini[23b,23a], S. Franchino[63a], D. Francis[36], L. Franco[112], L. Franconi[19], M. Franklin[61], G. Frattari[26], A.C. Freegard[93], P.M. Freeman[20], W.S. Freund[81b], N. Fritzsche[50], A. Froch[54], D. Froidevaux[36], J.A. Frost[125], Y. Fu[62a], M. Fujimoto[117], E. Fullana Torregrosa[161,*], J. Fuster[161], A. Gabrielli[23b,23a], A. Gabrielli[154], P. Gadow[48], G. Gagliardi[57b,57a], L.G. Gagnon[17a], G.E. Gallardo[125], E.J. Gallas[125], B.J. Gallop[133], R. Gamboa Goni[93], K.K. Gan[118], S. Ganguly[152], J. Gao[62a], Y. Gao[52], F.M. Garay Walls[136a,136b], B. Garcia[29,ad], C. García[161], J.E. García Navarro[161], J.A. García Pascual[14a], M. Garcia-Sciveres[17a], R.W. Gardner[39], D. Garg[79], R.B. Garg[142], S. Gargiulo[54], C.A. Garner[154],

JHEP06(2023)082

V. Garonne[29], S.J. Gasiorowski[137], P. Gaspar[81b], G. Gaudio[72a], V. Gautam[13], P. Gauzzi[74a,74b], I.L. Gavrilenko[37], A. Gavrilyuk[37], C. Gay[162], G. Gaycken[48], E.N. Gazis[10], A.A. Geanta[27b,27e], C.M. Gee[135], J. Geisen[97], M. Geisen[99], C. Gemme[57b], M.H. Genest[60], S. Gentile[74a,74b], S. George[94], W.F. George[20], T. Geralis[46], L.O. Gerlach[55], P. Gessinger-Befurt[36], M. Ghasemi Bostanabad[163], M. Ghneimat[140], A. Ghosal[140], A. Ghosh[158], A. Ghosh[7], B. Giacobbe[23b], S. Giagu[74a,74b], N. Giangiacomi[154], P. Giannetti[73a], A. Giannini[62a], S.M. Gibson[94], M. Gignac[135], D.T. Gil[84b], A.K. Gilbert[84a], B.J. Gilbert[41], D. Gillberg[34], G. Gilles[113], N.E.K. Gillwald[48], L. Ginabat[126], D.M. Gingrich[2,aa], M.P. Giordani[68a,68c], P.F. Giraud[134], G. Giugliarelli[68a,68c], D. Giugni[70a], F. Giuli[36], I. Gkialas[9,i], L.K. Gladilin[37], C. Glasman[98], G.R. Gledhill[122], M. Glisic[122], I. Gnesi[43b,e], Y. Go[29,ad], M. Goblirsch-Kolb[26], D. Godin[107], S. Goldfarb[104], T. Golling[56], M.G.D. Gololo[33g], D. Golubkov[37], J.P. Gombas[106], A. Gomes[129a,129b], G. Gomes Da Silva[140], A.J. Gomez Delegido[161], R. Goncalves Gama[55], R. Gonçalo[129a,129c], G. Gonella[122], L. Gonella[20], A. Gongadze[38], F. Gonnella[20], J.L. Gonski[41], R.Y. González Andana[52], S. González de la Hoz[161], S. Gonzalez Fernandez[13], R. Gonzalez Lopez[91], C. Gonzalez Renteria[17a], R. Gonzalez Suarez[159], S. Gonzalez-Sevilla[56], G.R. Gonzalvo Rodriguez[161], L. Goossens[36], N.A. Gorasia[20], P.A. Gorbounov[37], B. Gorini[36], E. Gorini[69a,69b], A. Gorišek[92], A.T. Goshaw[51], M.I. Gostkin[38], C.A. Gottardo[36], M. Gouighri[35b], V. Goumarre[48], A.G. Goussiou[137], N. Govender[33c], C. Goy[4], I. Grabowska-Bold[84a], K. Graham[34], E. Gramstad[124], S. Grancagnolo[18], M. Grandi[145], V. Gratchev[37,*], P.M. Gravila[27f], F.G. Gravili[69a,69b], H.M. Gray[17a], M. Greco[69a,69b], C. Grefe[24], I.M. Gregor[48], P. Grenier[142], C. Grieco[13], A.A. Grillo[135], K. Grimm[31,m], S. Grinstein[13,t], J.-F. Grivaz[66], E. Gross[167], J. Grosse-Knetter[55], C. Grud[105], A. Grummer[111], J.C. Grundy[125], L. Guan[105], W. Guan[168], C. Gubbels[162], J.G.R. Guerrero Rojas[161], G. Guerrieri[68a,68b], F. Guescini[109], R. Gugel[99], J.A.M. Guhit[105], A. Guida[48], T. Guillemin[4], E. Guilloton[165,133], S. Guindon[36], F. Guo[14a,14d], J. Guo[62c], L. Guo[66], Y. Guo[105], R. Gupta[48], S. Gurbuz[24], S.S. Gurdasani[54], G. Gustavino[36], M. Guth[56], P. Gutierrez[119], L.F. Gutierrez Zagazeta[127], C. Gutschow[95], C. Guyot[134], C. Gwenlan[125], C.B. Gwilliam[91], E.S. Haaland[124], A. Haas[116], M. Habedank[48], C. Haber[17a], H.K. Hadavand[8], A. Hadef[99], S. Hadzic[109], M. Haleem[164], J. Haley[120], J.J. Hall[138], G.D. Hallewell[101], L. Halser[19], K. Hamano[163], H. Hamdaoui[35e], M. Hamer[24], G.N. Hamity[52], J. Han[62b], K. Han[62a], L. Han[14c], L. Han[62a], S. Han[17a], Y.F. Han[154], K. Hanagaki[82], M. Hance[135], D.A. Hangal[41,y], M.D. Hank[39], R. Hankache[100], J.B. Hansen[42], J.D. Hansen[42], P.H. Hansen[42], K. Hara[156], D. Harada[56], T. Harenberg[169], S. Harkusha[37], Y.T. Harris[125], N.M. Harrison[118], P.F. Harrison[165], N.M. Hartman[142], N.M. Hartmann[108], Y. Hasegawa[139], A. Hasib[52], S. Haug[19], R. Hauser[106], M. Havranek[131], C.M. Hawkes[20], R.J. Hawkings[36], S. Hayashida[110], D. Hayden[106], C. Hayes[105], R.L. Hayes[162], C.P. Hays[125], J.M. Hays[93], H.S. Hayward[91], F. He[62a], Y. He[153], Y. He[126], M.P. Heath[52], V. Hedberg[97], A.L. Heggelund[124], N.D. Hehir[93], C. Heidegger[54], K.K. Heidegger[54], W.D. Heidorn[80], J. Heilman[34], S. Heim[48], T. Heim[17a], J.G. Heinlein[127],

JHEP06(2023)082

J.J. Heinrich[122], L. Heinrich[109], J. Hejbal[130], L. Helary[48], A. Held[168], S. Hellesund[124], C.M. Helling[162], S. Hellman[47a,47b], C. Helsens[36], R.C.W. Henderson[90], L. Henkelmann[32], A.M. Henriques Correia[36], H. Herde[142], Y. Hernández Jiménez[144], M.G. Herrmann[108], T. Herrmann[50], G. Herten[54], R. Hertenberger[108], L. Hervas[36], N.P. Hessey[155a], H. Hibi[83], E. Higón-Rodriguez[161], S.J. Hillier[20], I. Hinchliffe[17a], F. Hinterkeuser[24], M. Hirose[123], S. Hirose[156], D. Hirschbuehl[169], T.G. Hitchings[100], B. Hiti[92], J. Hobbs[144], R. Hobincu[27e], N. Hod[167], M.C. Hodgkinson[138], B.H. Hodkinson[32], A. Hoecker[36], J. Hofer[48], D. Hohn[54], T. Holm[24], M. Holzbock[109], L.B.A.H. Hommels[32], B.P. Honan[100], J. Hong[62c], T.M. Hong[128], Y. Hong[55], J.C. Honig[54], A. Hönle[109], B.H. Hooberman[160], W.H. Hopkins[6], Y. Horii[110], S. Hou[147], A.S. Howard[92], J. Howarth[59], J. Hoya[6], M. Hrabovsky[121], A. Hrynevich[37], T. Hryn'ova[4], P.J. Hsu[65], S.-C. Hsu[137], Q. Hu[41,y], Y.F. Hu[14a,14d,ac], D.P. Huang[95], S. Huang[64b], X. Huang[14c], Y. Huang[62a], Y. Huang[14a], Z. Huang[100], Z. Hubacek[131], M. Huebner[24], F. Huegging[24], T.B. Huffman[125], M. Huhtinen[36], S.K. Huiberts[16], R. Hulsken[103], N. Huseynov[12,a], J. Huston[106], J. Huth[61], R. Hyneman[142], S. Hyrych[28a], G. Iacobucci[56], G. Iakovidis[29], I. Ibragimov[140], L. Iconomidou-Fayard[66], P. Iengo[71a,71b], R. Iguchi[152], T. Iizawa[56], Y. Ikegami[82], A. Ilg[19], N. Ilic[154], H. Imam[35a], T. Ingebretsen Carlson[47a,47b], G. Introzzi[72a,72b], M. Iodice[76a], V. Ippolito[74a,74b], M. Ishino[152], W. Islam[168], C. Issever[18,48], S. Istin[21a,af], H. Ito[166], J.M. Iturbe Ponce[64a], R. Iuppa[77a,77b], A. Ivina[167], J.M. Izen[45], V. Izzo[71a], P. Jacka[130,131], P. Jackson[1], R.M. Jacobs[48], B.P. Jaeger[141], C.S. Jagfeld[108], G. Jäkel[169], K. Jakobs[54], T. Jakoubek[167], J. Jamieson[59], K.W. Janas[84a], G. Jarlskog[97], A.E. Jaspan[91], M. Javurkova[102], F. Jeanneau[134], L. Jeanty[122], J. Jejelava[148a,x], P. Jenni[54,f], C.E. Jessiman[34], S. Jézéquel[4], J. Jia[144], X. Jia[61], X. Jia[14a,14d], Z. Jia[14c], Y. Jiang[62a], S. Jiggins[52], J. Jimenez Pena[109], S. Jin[14c], A. Jinaru[27b], O. Jinnouchi[153], P. Johansson[138], K.A. Johns[7], D.M. Jones[32], E. Jones[165], P. Jones[32], R.W.L. Jones[90], T.J. Jones[91], R. Joshi[118], J. Jovicevic[15], X. Ju[17a], J.J. Junggeburth[36], A. Juste Rozas[13,t], S. Kabana[136e], A. Kaczmarska[85], M. Kado[74a,74b], H. Kagan[118], M. Kagan[142], A. Kahn[41], A. Kahn[127], C. Kahra[99], T. Kaji[166], E. Kajomovitz[149], N. Kakati[167], C.W. Kalderon[29], A. Kamenshchikov[154], S. Kanayama[153], N.J. Kang[135], Y. Kano[110], D. Kar[33g], K. Karava[125], M.J. Kareem[155b], E. Karentzos[54], I. Karkanias[151], S.N. Karpov[38], Z.M. Karpova[38], V. Kartvelishvili[90], A.N. Karyukhin[37], E. Kasimi[151], C. Kato[62d], J. Katzy[48], S. Kaur[34], K. Kawade[139], K. Kawagoe[88], T. Kawamoto[134], G. Kawamura[55], E.F. Kay[163], F.I. Kaya[157], S. Kazakos[13], V.F. Kazanin[37], Y. Ke[144], J.M. Keaveney[33a], R. Keeler[163], G.V. Kehris[61], J.S. Keller[34], A.S. Kelly[95], D. Kelsey[145], J.J. Kempster[20], K.E. Kennedy[41], O. Kepka[130], B.P. Kerridge[165], S. Kersten[169], B.P. Kerševan[92], S. Keshri[66], L. Keszeghova[28a], S. Ketabchi Haghighat[154], M. Khandoga[126], A. Khanov[120], A.G. Kharlamov[37], T. Kharlamova[37], E.E. Khoda[137], T.J. Khoo[18], G. Khoriauli[164], J. Khubua[148b], Y.A.R. Khwaira[66], M. Kiehn[36], A. Kilgallon[122], D.W. Kim[47a,47b], E. Kim[153], Y.K. Kim[39], N. Kimura[95], A. Kirchhoff[55], D. Kirchmeier[50], C. Kirfel[24], J. Kirk[133], A.E. Kiryunin[109], T. Kishimoto[152], D.P. Kisliuk[154], C. Kitsaki[10], O. Kivernyk[24],

JHEP06(2023)082

M. Klassen[63a], C. Klein[34], L. Klein[164], M.H. Klein[105], M. Klein[91], S.B. Klein[56], U. Klein[91], P. Klimek[36], A. Klimentov[29], F. Klimpel[109], T. Klingl[24], T. Klioutchnikova[36], F.F. Klitzner[108], P. Kluit[113], S. Kluth[109], E. Kneringer[78], T.M. Knight[154], A. Knue[54], D. Kobayashi[88], R. Kobayashi[86], M. Kocian[142], P. Kodyš[132], D.M. Koeck[145], P.T. Koenig[24], T. Koffas[34], N.M. Köhler[36], M. Kolb[134], I. Koletsou[4], T. Komarek[121], K. Köneke[54], A.X.Y. Kong[1], T. Kono[117], N. Konstantinidis[95], B. Konya[97], R. Kopeliansky[67], S. Koperny[84a], K. Korcyl[85], K. Kordas[151], G. Koren[150], A. Korn[95], S. Korn[55], I. Korolkov[13], N. Korotkova[37], B. Kortman[113], O. Kortner[109], S. Kortner[109], W.H. Kostecka[114], V.V. Kostyukhin[140], A. Kotsokechagia[134], A. Kotwal[51], A. Koulouris[36], A. Kourkoumeli-Charalampidi[72a,72b], C. Kourkoumelis[9], E. Kourlitis[6], O. Kovanda[145], R. Kowalewski[163], W. Kozanecki[134], A.S. Kozhin[37], V.A. Kramarenko[37], G. Kramberger[92], P. Kramer[99], M.W. Krasny[126], A. Krasznahorkay[36], J.A. Kremer[99], T. Kresse[50], J. Kretzschmar[91], K. Kreul[18], P. Krieger[154], F. Krieter[108], S. Krishnamurthy[102], A. Krishnan[63b], M. Krivos[132], K. Krizka[17a], K. Kroeninger[49], H. Kroha[109], J. Kroll[130], J. Kroll[127], K.S. Krowpman[106], U. Kruchonak[38], H. Krüger[24], N. Krumnack[80], M.C. Kruse[51], J.A. Krzysiak[85], A. Kubota[153], O. Kuchinskaia[37], S. Kuday[3a], D. Kuechler[48], J.T. Kuechler[48], S. Kuehn[36], T. Kuhl[48], V. Kukhtin[38], Y. Kulchitsky[37,a], S. Kuleshov[136d,136b], M. Kumar[33g], N. Kumari[101], M. Kuna[60], A. Kupco[130], T. Kupfer[49], A. Kupich[37], O. Kuprash[54], H. Kurashige[83], L.L. Kurchaninov[155a], Y.A. Kurochkin[37], A. Kurova[37], E.S. Kuwertz[36], M. Kuze[153], A.K. Kvam[102], J. Kvita[121], T. Kwan[103], K.W. Kwok[64a], N.G. Kyriacou[105], L.A.O. Laatu[101], C. Lacasta[161], F. Lacava[74a,74b], H. Lacker[18], D. Lacour[126], N.N. Lad[95], E. Ladygin[38], B. Laforge[126], T. Lagouri[136e], S. Lai[55], I.K. Lakomiec[84a], N. Lalloue[60], J.E. Lambert[119], S. Lammers[67], W. Lampl[7], C. Lampoudis[151], A.N. Lancaster[114], E. Lançon[29], U. Landgraf[54], M.P.J. Landon[93], V.S. Lang[54], R.J. Langenberg[102], A.J. Lankford[158], F. Lanni[36], K. Lantzsch[24], A. Lanza[72a], A. Lapertosa[57b,57a], J.F. Laporte[134], T. Lari[70a], F. Lasagni Manghi[23b], M. Lassnig[36], V. Latonova[130], T.S. Lau[64a], A. Laudrain[99], A. Laurier[34], S.D. Lawlor[94], Z. Lawrence[100], M. Lazzaroni[70a,70b], B. Le[100], B. Leban[92], A. Lebedev[80], M. LeBlanc[36], T. LeCompte[6], F. Ledroit-Guillon[60], A.C.A. Lee[95], G.R. Lee[16], L. Lee[61], S.C. Lee[147], S. Lee[47a,47b], T.F. Lee[91], L.L. Leeuw[33c], H.P. Lefebvre[94], M. Lefebvre[163], C. Leggett[17a], K. Lehmann[141], G. Lehmann Miotto[36], M. Leigh[56], W.A. Leight[102], A. Leisos[151,s], M.A.L. Leite[81c], C.E. Leitgeb[48], R. Leitner[132], K.J.C. Leney[44], T. Lenz[24], S. Leone[73a], C. Leonidopoulos[52], A. Leopold[143], C. Leroy[107], R. Les[106], C.G. Lester[32], M. Levchenko[37], J. Levêque[4], D. Levin[105], L.J. Levinson[167], M.P. Lewicki[85], D.J. Lewis[20], B. Li[14b], B. Li[62b], C. Li[62a], C-Q. Li[62c,62d], H. Li[62a], H. Li[62b], H. Li[14c], H. Li[62b], J. Li[62c], K. Li[137], L. Li[62c], M. Li[14a,14d], Q.Y. Li[62a], S. Li[62d,62c,d], T. Li[62b], X. Li[103], Z. Li[62b], Z. Li[125], Z. Li[103], Z. Li[91], Z. Liang[14a], M. Liberatore[48], B. Liberti[75a], K. Lie[64c], J. Lieber Marin[81b], K. Lin[106], R.A. Linck[67], R.E. Lindley[7], J.H. Lindon[2], A. Linss[48], E. Lipeles[127], A. Lipniacka[16], A. Lister[162], J.D. Little[4], B. Liu[14a], B.X. Liu[141], D. Liu[62d,62c], J.B. Liu[62a], J.K.K. Liu[32], K. Liu[62d,62c], M. Liu[62a], M.Y. Liu[62a], P. Liu[14a], Q. Liu[62d,137,62c],

JHEP06(2023)082

X. Liu[62a], Y. Liu[48], Y. Liu[14c,14d], Y.L. Liu[105], Y.W. Liu[62a], M. Livan[72a,72b], J. Llorente Merino[141], S.L. Lloyd[93], E.M. Lobodzinska[48], P. Loch[7], S. Loffredo[75a,75b], T. Lohse[18], K. Lohwasser[138], M. Lokajicek[130], J.D. Long[160], I. Longarini[74a,74b], L. Longo[69a,69b], R. Longo[160], I. Lopez Paz[36], A. Lopez Solis[48], J. Lorenz[108], N. Lorenzo Martinez[4], A.M. Lory[108], A. Lösle[54], X. Lou[47a,47b], X. Lou[14a,14d], A. Lounis[66], J. Love[6], P.A. Love[90], J.J. Lozano Bahilo[161], G. Lu[14a,14d], M. Lu[79], S. Lu[127], Y.J. Lu[65], H.J. Lubatti[137], C. Luci[74a,74b], F.L. Lucio Alves[14c], A. Lucotte[60], F. Luehring[67], I. Luise[144], O. Lukianchuk[66], O. Lundberg[143], B. Lund-Jensen[143], N.A. Luongo[122], M.S. Lutz[150], D. Lynn[29], H. Lyons[91], R. Lysak[130], E. Lytken[97], F. Lyu[14a], V. Lyubushkin[38], T. Lyubushkina[38], H. Ma[29], L.L. Ma[62b], Y. Ma[95], D.M. Mac Donell[163], G. Maccarrone[53], J.C. MacDonald[138], R. Madar[40], W.F. Mader[50], J. Maeda[83], T. Maeno[29], M. Maerker[50], V. Magerl[54], J. Magro[68a,68c], H. Maguire[138], D.J. Mahon[41], C. Maidantchik[81b], A. Maio[129a,129b,129d], K. Maj[84a], O. Majersky[28a], S. Majewski[122], N. Makovec[66], V. Maksimovic[15], B. Malaescu[126], Pa. Malecki[85], V.P. Maleev[37], F. Malek[60], D. Malito[43b,43a], U. Mallik[79], C. Malone[32], S. Maltezos[10], S. Malyukov[38], J. Mamuzic[13], G. Mancini[53], G. Manco[72a,72b], J.P. Mandalia[93], I. Mandić[92], L. Manhaes de Andrade Filho[81a], I.M. Maniatis[151], M. Manisha[134], J. Manjarres Ramos[50], D.C. Mankad[167], A. Mann[108], B. Mansoulie[134], S. Manzoni[36], A. Marantis[151], G. Marchiori[5], M. Marcisovsky[130], L. Marcoccia[75a,75b], C. Marcon[70a,70b], M. Marinescu[20], M. Marjanovic[119], Z. Marshall[17a], S. Marti-Garcia[161], T.A. Martin[165], V.J. Martin[52], B. Martin dit Latour[16], L. Martinelli[74a,74b], M. Martinez[13,t], P. Martinez Agullo[161], V.I. Martinez Outschoorn[102], P. Martinez Suarez[13], S. Martin-Haugh[133], V.S. Martoiu[27b], A.C. Martyniuk[95], A. Marzin[36], S.R. Maschek[109], L. Masetti[99], T. Mashimo[152], J. Masik[100], A.L. Maslennikov[37], L. Massa[23b], P. Massarotti[71a,71b], P. Mastrandrea[73a,73b], A. Mastroberardino[43b,43a], T. Masubuchi[152], T. Mathisen[159], N. Matsuzawa[152], J. Maurer[27b], B. Maček[92], D.A. Maximov[37], R. Mazini[147], I. Maznas[151], M. Mazza[106], S.M. Mazza[135], C. Mc Ginn[29,ad], J.P. Mc Gowan[103], S.P. Mc Kee[105], T.G. McCarthy[109], W.P. McCormack[17a], E.F. McDonald[104], A.E. McDougall[113], J.A. Mcfayden[145], G. Mchedlidze[148b], R.P. Mckenzie[33g], T.C. Mclachlan[48], D.J. Mclaughlin[95], K.D. McLean[163], S.J. McMahon[133], P.C. McNamara[104], C.M. Mcpartland[91], R.A. McPherson[163,v], T. Megy[40], S. Mehlhase[108], A. Mehta[91], B. Meirose[45], D. Melini[149], B.R. Mellado Garcia[33g], A.H. Melo[55], F. Meloni[48], E.D. Mendes Gouveia[129a], A.M. Mendes Jacques Da Costa[20], H.Y. Meng[154], L. Meng[90], S. Menke[109], M. Mentink[36], E. Meoni[43b,43a], C. Merlassino[125], L. Merola[71a,71b], C. Meroni[70a], G. Merz[105], O. Meshkov[37], J.K.R. Meshreki[140], J. Metcalfe[6], A.S. Mete[6], C. Meyer[67], J-P. Meyer[134], M. Michetti[18], R.P. Middleton[133], L. Mijović[52], G. Mikenberg[167], M. Mikestikova[130], M. Mikuž[92], H. Mildner[138], A. Milic[154], C.D. Milke[44], D.W. Miller[39], L.S. Miller[34], A. Milov[167], D.A. Milstead[47a,47b], T. Min[14c], A.A. Minaenko[37], I.A. Minashvili[148b], L. Mince[59], A.I. Mincer[116], B. Mindur[84a], M. Mineev[38], Y. Mino[86], L.M. Mir[13], M. Miralles Lopez[161], M. Mironova[125], T. Mitani[166], A. Mitra[165], V.A. Mitsou[161], O. Miu[154], P.S. Miyagawa[93], Y. Miyazaki[88], A. Mizukami[82], J.U. Mjörnmark[97],

JHEP06(2023)082

T. Mkrtchyan[63a], T. Mlinarevic[95], M. Mlynarikova[36], T. Moa[47a,47b], S. Mobius[55], K. Mochizuki[107], P. Moder[48], P. Mogg[108], A.F. Mohammed[14a,14d], S. Mohapatra[41], G. Mokgatitswane[33g], B. Mondal[140], S. Mondal[131], K. Mönig[48], E. Monnier[101], L. Monsonis Romero[161], J. Montejo Berlingen[36], M. Montella[118], F. Monticelli[89], N. Morange[66], A.L. Moreira De Carvalho[129a], M. Moreno Llácer[161], C. Moreno Martinez[13], P. Morettini[57b], S. Morgenstern[165], M. Morii[61], M. Morinaga[152], V. Morisbak[124], A.K. Morley[36], F. Morodei[74a,74b], L. Morvaj[36], P. Moschovakos[36], B. Moser[36], M. Mosidze[148b], T. Moskalets[54], P. Moskvitina[112], J. Moss[31,n], E.J.W. Moyse[102], S. Muanza[101], J. Mueller[128], D. Muenstermann[90], R. Müller[19], G.A. Mullier[97], J.J. Mullin[127], D.P. Mungo[70a,70b], J.L. Munoz Martinez[13], D. Munoz Perez[161], F.J. Munoz Sanchez[100], M. Murin[100], W.J. Murray[165,133], A. Murrone[70a,70b], J.M. Muse[119], M. Muškinja[17a], C. Mwewa[29], A.G. Myagkov[37,a], A.J. Myers[8], A.A. Myers[128], G. Myers[67], M. Myska[131], B.P. Nachman[17a], O. Nackenhorst[49], A. Nag[50], K. Nagai[125], K. Nagano[82], J.L. Nagle[29,ad], E. Nagy[101], A.M. Nairz[36], Y. Nakahama[82], K. Nakamura[82], H. Nanjo[123], R. Narayan[44], E.A. Narayanan[111], I. Naryshkin[37], M. Naseri[34], C. Nass[24], G. Navarro[22a], J. Navarro-Gonzalez[161], R. Nayak[150], A. Nayaz[18], P.Y. Nechaeva[37], F. Nechansky[48], L. Nedic[125], T.J. Neep[20], A. Negri[72a,72b], M. Negrini[23b], C. Nellist[112], C. Nelson[103], K. Nelson[105], S. Nemecek[130], M. Nessi[36,g], M.S. Neubauer[160], F. Neuhaus[99], J. Neundorf[48], R. Newhouse[162], P.R. Newman[20], C.W. Ng[128], Y.S. Ng[18], Y.W.Y. Ng[158], B. Ngair[35e], H.D.N. Nguyen[107], R.B. Nickerson[125], R. Nicolaidou[134], J. Nielsen[135], M. Niemeyer[55], N. Nikiforou[36], V. Nikolaenko[37,a], I. Nikolic-Audit[126], K. Nikolopoulos[20], P. Nilsson[29], H.R. Nindhito[56], A. Nisati[74a], N. Nishu[2], R. Nisius[109], J-E. Nitschke[50], E.K. Nkadimeng[33g], S.J. Noacco Rosende[89], T. Nobe[152], D.L. Noel[32], Y. Noguchi[86], T. Nommensen[146], M.A. Nomura[29], M.B. Norfolk[138], R.R.B. Norisam[95], B.J. Norman[34], J. Novak[92], T. Novak[48], O. Novgorodova[50], L. Novotny[131], R. Novotny[111], L. Nozka[121], K. Ntekas[158], E. Nurse[95], F.G. Oakham[34,aa], J. Ocariz[126], A. Ochi[83], I. Ochoa[129a], S. Oerdek[159], A. Ogrodnik[84a], A. Oh[100], C.C. Ohm[143], H. Oide[153], R. Oishi[152], M.L. Ojeda[48], Y. Okazaki[86], M.W. O'Keefe[91], Y. Okumura[152], A. Olariu[27b], L.F. Oleiro Seabra[129a], S.A. Olivares Pino[136e], D. Oliveira Damazio[29], D. Oliveira Goncalves[81a], J.L. Oliver[158], M.J.R. Olsson[158], A. Olszewski[85], J. Olszowska[85,*], Ö.O. Öncel[54], D.C. O'Neil[141], A.P. O'Neill[19], A. Onofre[129a,129e], P.U.E. Onyisi[11], M.J. Oreglia[39], G.E. Orellana[89], D. Orestano[76a,76b], N. Orlando[13], R.S. Orr[154], V. O'Shea[59], R. Ospanov[62a], G. Otero y Garzon[30], H. Otono[88], P.S. Ott[63a], G.J. Ottino[17a], M. Ouchrif[35d], J. Ouellette[29,ad], F. Ould-Saada[124], M. Owen[59], R.E. Owen[133], K.Y. Oyulmaz[21a], V.E. Ozcan[21a], N. Ozturk[8], S. Ozturk[21d], J. Pacalt[121], H.A. Pacey[32], K. Pachal[51], A. Pacheco Pages[13], C. Padilla Aranda[13], G. Padovano[74a,74b], S. Pagan Griso[17a], G. Palacino[67], A. Palazzo[69a,69b], S. Palazzo[52], S. Palestini[36], M. Palka[84b], J. Pan[170], T. Pan[64a], D.K. Panchal[11], C.E. Pandini[113], J.G. Panduro Vazquez[94], H. Pang[14b], P. Pani[48], G. Panizzo[68a,68c], L. Paolozzi[56], C. Papadatos[107], S. Parajuli[44], A. Paramonov[6], C. Paraskevopoulos[10], D. Paredes Hernandez[64b], T.H. Park[154], M.A. Parker[32], F. Parodi[57b,57a], E.W. Parrish[114], V.A. Parrish[52], J.A. Parsons[41],

JHEP06(2023)082

U. Parzefall[54], B. Pascual Dias[107], L. Pascual Dominguez[150], V.R. Pascuzzi[17a], F. Pasquali[113], E. Pasqualucci[74a], S. Passaggio[57b], F. Pastore[94], P. Pasuwan[47a,47b], P. Patel[85], J.R. Pater[100], J. Patton[91], T. Pauly[36], J. Pearkes[142], M. Pedersen[124], R. Pedro[129a], S.V. Peleganchuk[37], O. Penc[36], E.A. Pender[52], C. Peng[64b], H. Peng[62a], K.E. Penski[108], M. Penzin[37], B.S. Peralva[81d,81d], A.P. Pereira Peixoto[60], L. Pereira Sanchez[47a,47b], D.V. Perepelitsa[29,ad], E. Perez Codina[155a], M. Perganti[10], L. Perini[70a,70b,*], H. Pernegger[36], S. Perrella[36], A. Perrevoort[112], O. Perrin[40], K. Peters[48], R.F.Y. Peters[100], B.A. Petersen[36], T.C. Petersen[42], E. Petit[101], V. Petousis[131], C. Petridou[151], A. Petrukhin[140], M. Pettee[17a], N.E. Pettersson[36], A. Petukhov[37], K. Petukhova[132], A. Peyaud[134], R. Pezoa[136f], L. Pezzotti[36], G. Pezzullo[170], T.M. Pham[168], T. Pham[104], P.W. Phillips[133], M.W. Phipps[160], G. Piacquadio[144], E. Pianori[17a], F. Piazza[70a,70b], R. Piegaia[30], D. Pietreanu[27b], A.D. Pilkington[100], M. Pinamonti[68a,68c], J.L. Pinfold[2], B.C. Pinheiro Pereira[129a], C. Pitman Donaldson[95], D.A. Pizzi[34], L. Pizzimento[75a,75b], A. Pizzini[113], M.-A. Pleier[29], V. Plesanovs[54], V. Pleskot[132], E. Plotnikova[38], G. Poddar[4], R. Poettgen[97], L. Poggioli[126], I. Pogrebnyak[106], D. Pohl[24], I. Pokharel[55], S. Polacek[132], G. Polesello[72a], A. Poley[141,155a], R. Polifka[131], A. Polini[23b], C.S. Pollard[125], Z.B. Pollock[118], V. Polychronakos[29], E. Pompa Pacchi[74a,74b], D. Ponomarenko[37], L. Pontecorvo[36], S. Popa[27a], G.A. Popeneciu[27d], D.M. Portillo Quintero[155a], S. Pospisil[131], P. Postolache[27c], K. Potamianos[125], I.N. Potrap[38], C.J. Potter[32], H. Potti[1], T. Poulsen[48], J. Poveda[161], G. Pownall[48], M.E. Pozo Astigarraga[36], A. Prades Ibanez[161], M.M. Prapa[46], D. Price[100], M. Primavera[69a], M.A. Principe Martin[98], M.L. Proffitt[137], N. Proklova[127], K. Prokofiev[64c], G. Proto[75a,75b], S. Protopopescu[29], J. Proudfoot[6], M. Przybycien[84a], J.E. Puddefoot[138], D. Pudzha[37], P. Puzo[66], D. Pyatiizbyantseva[37], J. Qian[105], Y. Qin[100], T. Qiu[93], A. Quadt[55], M. Queitsch-Maitland[100], G. Rabanal Bolanos[61], D. Rafanoharana[54], F. Ragusa[70a,70b], J.L. Rainbolt[39], J.A. Raine[56], S. Rajagopalan[29], E. Ramakoti[37], K. Ran[48,14d], V. Raskina[126], D.F. Rassloff[63a], S. Rave[99], B. Ravina[55], I. Ravinovich[167], M. Raymond[36], A.L. Read[124], N.P. Readioff[138], D.M. Rebuzzi[72a,72b], G. Redlinger[29], K. Reeves[45], J.A. Reidelsturz[169], D. Reikher[150], A. Reiss[99], A. Rej[140], C. Rembser[36], A. Renardi[48], M. Renda[27b], M.B. Rendel[109], A.G. Rennie[59], S. Resconi[70a], M. Ressegotti[57b,57a], E.D. Resseguie[17a], S. Rettie[95], B. Reynolds[118], E. Reynolds[17a], M. Rezaei Estabragh[169], O.L. Rezanova[37], P. Reznicek[132], E. Ricci[77a,77b], R. Richter[109], S. Richter[47a,47b], E. Richter-Was[84b], M. Ridel[126], P. Rieck[116], P. Riedler[36], M. Rijssenbeek[144], A. Rimoldi[72a,72b], M. Rimoldi[48], L. Rinaldi[23b,23a], T.T. Rinn[29], M.P. Rinnagel[108], G. Ripellino[143], I. Riu[13], P. Rivadeneira[48], J.C. Rivera Vergara[163], F. Rizatdinova[120], E. Rizvi[93], C. Rizzi[56], B.A. Roberts[165], B.R. Roberts[17a], S.H. Robertson[103,v], M. Robin[48], D. Robinson[32], C.M. Robles Gajardo[136f], M. Robles Manzano[99], A. Robson[59], A. Rocchi[75a,75b], C. Roda[73a,73b], S. Rodriguez Bosca[63a], Y. Rodriguez Garcia[22a], A. Rodriguez Rodriguez[54], A.M. Rodríguez Vera[155b], S. Roe[36], J.T. Roemer[158], A.R. Roepe-Gier[119], J. Roggel[169], O. Røhne[124], R.A. Rojas[163], B. Roland[54], C.P.A. Roland[67], J. Roloff[29], A. Romaniouk[37], E. Romano[72a,72b], M. Romano[23b],

JHEP06(2023)082

A.C. Romero Hernandez[160], N. Rompotis[91], L. Roos[126], S. Rosati[74a], B.J. Rosser[39], E. Rossi[4], E. Rossi[71a,71b], L.P. Rossi[57b], L. Rossini[48], R. Rosten[118], M. Rotaru[27b], B. Rottler[54], D. Rousseau[66], D. Rousso[32], G. Rovelli[72a,72b], A. Roy[160], A. Rozanov[101], Y. Rozen[149], X. Ruan[33g], A. Rubio Jimenez[161], A.J. Ruby[91], V.H. Ruelas Rivera[18], T.A. Ruggeri[1], F. Rühr[54], A. Ruiz-Martinez[161], A. Rummler[36], Z. Rurikova[54], N.A. Rusakovich[38], H.L. Russell[163], J.P. Rutherfoord[7], K. Rybacki[90], M. Rybar[132], E.B. Rye[124], A. Ryzhov[37], J.A. Sabater Iglesias[56], P. Sabatini[161], L. Sabetta[74a,74b], H.F-W. Sadrozinski[135], F. Safai Tehrani[74a], B. Safarzadeh Samani[145], M. Safdari[142], S. Saha[103], M. Sahinsoy[109], M. Saimpert[134], M. Saito[152], T. Saito[152], D. Salamani[36], G. Salamanna[76a,76b], A. Salnikov[142], J. Salt[161], A. Salvador Salas[13], D. Salvatore[43b,43a], F. Salvatore[145], A. Salzburger[36], D. Sammel[54], D. Sampsonidis[151], D. Sampsonidou[62d,62c], J. Sánchez[161], A. Sanchez Pineda[4], V. Sanchez Sebastian[161], H. Sandaker[124], C.O. Sander[48], J.A. Sandesara[102], M. Sandhoff[169], C. Sandoval[22b], D.P.C. Sankey[133], A. Sansoni[53], L. Santi[74a,74b], C. Santoni[40], H. Santos[129a,129b], S.N. Santpur[17a], A. Santra[167], K.A. Saoucha[138], J.G. Saraiva[129a,129d], J. Sardain[7], O. Sasaki[82], K. Sato[156], C. Sauer[63b], F. Sauerburger[54], E. Sauvan[4], P. Savard[154,aa], R. Sawada[152], C. Sawyer[133], L. Sawyer[96], I. Sayago Galvan[161], C. Sbarra[23b], A. Sbrizzi[23b,23a], T. Scanlon[95], J. Schaarschmidt[137], P. Schacht[109], D. Schaefer[39], U. Schäfer[99], A.C. Schaffer[66], D. Schaile[108], R.D. Schamberger[144], E. Schanet[108], C. Scharf[18], V.A. Schegelsky[37], D. Scheirich[132], F. Schenck[18], M. Schernau[158], C. Scheulen[55], C. Schiavi[57b,57a], Z.M. Schillaci[26], E.J. Schioppa[69a,69b], M. Schioppa[43b,43a], B. Schlag[99], K.E. Schleicher[54], S. Schlenker[36], K. Schmieden[99], C. Schmitt[99], S. Schmitt[48], L. Schoeffel[134], A. Schoening[63b], P.G. Scholer[54], E. Schopf[125], M. Schott[99], J. Schovancova[36], S. Schramm[56], F. Schroeder[169], H-C. Schultz-Coulon[63a], M. Schumacher[54], B.A. Schumm[135], Ph. Schune[134], A. Schwartzman[142], T.A. Schwarz[105], Ph. Schwemling[134], R. Schwienhorst[106], A. Sciandra[135], G. Sciolla[26], F. Scuri[73a], F. Scutti[104], C.D. Sebastiani[91], K. Sedlaczek[49], P. Seema[18], S.C. Seidel[111], A. Seiden[135], B.D. Seidlitz[41], T. Seiss[39], C. Seitz[48], J.M. Seixas[81b], G. Sekhniaidze[71a], S.J. Sekula[44], L. Selem[4], N. Semprini-Cesari[23b,23a], A. Semushin[37], S. Sen[51], D. Sengupta[56], V. Senthilkumar[161], L. Serin[66], L. Serkin[68a,68b], M. Sessa[76a,76b], H. Severini[119], S. Sevova[142], F. Sforza[57b,57a], A. Sfyrla[56], E. Shabalina[55], R. Shaheen[143], J.D. Shahinian[127], N.W. Shaikh[47a,47b], D. Shaked Renous[167], L.Y. Shan[14a], M. Shapiro[17a], A. Sharma[36], A.S. Sharma[162], P. Sharma[79], S. Sharma[48], P.B. Shatalov[37], K. Shaw[145], S.M. Shaw[100], Q. Shen[62c,5], P. Sherwood[95], L. Shi[95], C.O. Shimmin[170], Y. Shimogama[166], J.D. Shinner[94], I.P.J. Shipsey[125], S. Shirabe[60], M. Shiyakova[38], J. Shlomi[167], M.J. Shochet[39], J. Shojaii[104], D.R. Shope[124], S. Shrestha[118,ae], E.M. Shrif[33g], M.J. Shroff[163], P. Sicho[130], A.M. Sickles[160], E. Sideras Haddad[33g], A. Sidoti[23b], F. Siegert[50], Dj. Sijacki[15], R. Sikora[84a], F. Sili[89], J.M. Silva[20], M.V. Silva Oliveira[36], S.B. Silverstein[47a], S. Simion[66], R. Simoniello[36], E.L. Simpson[59], N.D. Simpson[97], S. Simsek[21d], S. Sindhu[55], P. Sinervo[154], V. Sinetckii[37], S. Singh[141], S. Singh[154], S. Sinha[48], S. Sinha[33g], M. Sioli[23b,23a], I. Siral[122], S.Yu. Sivoklokov[37,*], J. Sjölin[47a,47b], A. Skaf[55], E. Skorda[97], P. Skubic[119], M. Slawinska[85], V. Smakhtin[167],

JHEP06(2023)082

B.H. Smart[133], J. Smiesko[36], S.Yu. Smirnov[37], Y. Smirnov[37], L.N. Smirnova[37,a], O. Smirnova[97], A.C. Smith[41], E.A. Smith[39], H.A. Smith[125], J.L. Smith[91], R. Smith[142], M. Smizanska[90], K. Smolek[131], A. Smykiewicz[85], A.A. Snesarev[37], H.L. Snoek[113], S. Snyder[29], R. Sobie[163,v], A. Soffer[150], C.A. Solans Sanchez[36], E.Yu. Soldatov[37], U. Soldevila[161], A.A. Solodkov[37], S. Solomon[54], A. Soloshenko[38], K. Solovieva[54], O.V. Solovyanov[37], V. Solovyev[37], P. Sommer[36], A. Sonay[13], W.Y. Song[155b], A. Sopczak[131], A.L. Sopio[95], F. Sopkova[28b], V. Sothilingam[63a], S. Sottocornola[72a,72b], R. Soualah[115c], Z. Soumaimi[35e], D. South[48], S. Spagnolo[69a,69b], M. Spalla[109], F. Spanò[94], D. Sperlich[54], G. Spigo[36], M. Spina[145], S. Spinali[90], D.P. Spiteri[59], M. Spousta[132], E.J. Staats[34], A. Stabile[70a,70b], R. Stamen[63a], M. Stamenkovic[113], A. Stampekis[20], M. Standke[24], E. Stanecka[85], M.V. Stange[50], B. Stanislaus[17a], M.M. Stanitzki[48], M. Stankaityte[125], B. Stapf[48], E.A. Starchenko[37], G.H. Stark[135], J. Stark[101], D.M. Starko[155b], P. Staroba[130], P. Starovoitov[63a], S. Stärz[103], R. Staszewski[85], G. Stavropoulos[46], J. Steentoft[159], P. Steinberg[29], A.L. Steinhebel[122], B. Stelzer[141,155a], H.J. Stelzer[128], O. Stelzer-Chilton[155a], H. Stenzel[58], T.J. Stevenson[145], G.A. Stewart[36], M.C. Stockton[36], G. Stoicea[27b], M. Stolarski[129a], S. Stonjek[109], A. Straessner[50], J. Strandberg[143], S. Strandberg[47a,47b], M. Strauss[119], T. Strebler[101], P. Strizenec[28b], R. Ströhmer[164], D.M. Strom[122], L.R. Strom[48], R. Stroynowski[44], A. Strubig[47a,47b], S.A. Stucci[29], B. Stugu[16], J. Stupak[119], N.A. Styles[48], D. Su[142], S. Su[62a], W. Su[62d,137,62c], X. Su[62a,66], K. Sugizaki[152], V.V. Sulin[37], M.J. Sullivan[91], D.M.S. Sultan[77a,77b], L. Sultanaliyeva[37], S. Sultansoy[3b], T. Sumida[86], S. Sun[105], S. Sun[168], O. Sunneborn Gudnadottir[159], M.R. Sutton[145], M. Svatos[130], M. Swiatlowski[155a], T. Swirski[164], I. Sykora[28a], M. Sykora[132], T. Sykora[132], D. Ta[99], K. Tackmann[48,u], A. Taffard[158], R. Tafirout[155a], J.S. Tafoya Vargas[66], R.H.M. Taibah[126], R. Takashima[87], K. Takeda[83], E.P. Takeva[52], Y. Takubo[82], M. Talby[101], A.A. Talyshev[37], K.C. Tam[64b], N.M. Tamir[150], A. Tanaka[152], J. Tanaka[152], R. Tanaka[66], M. Tanasini[57b,57a], J. Tang[62c], Z. Tao[162], S. Tapia Araya[80], S. Tapprogge[99], A. Tarek Abouelfadl Mohamed[106], S. Tarem[149], K. Tariq[62b], G. Tarna[27b], G.F. Tartarelli[70a], P. Tas[132], M. Tasevsky[130], E. Tassi[43b,43a], A.C. Tate[160], G. Tateno[152], Y. Tayalati[35e], G.N. Taylor[104], W. Taylor[155b], H. Teagle[91], A.S. Tee[168], R. Teixeira De Lima[142], P. Teixeira-Dias[94], J.J. Teoh[154], K. Terashi[152], J. Terron[98], S. Terzo[13], M. Testa[53], R.J. Teuscher[154,v], A. Thaler[78], O. Theiner[56], N. Themistokleous[52], T. Theveneaux-Pelzer[18], O. Thielmann[169], D.W. Thomas[94], J.P. Thomas[20], E.A. Thompson[48], P.D. Thompson[20], E. Thomson[127], E.J. Thorpe[93], Y. Tian[55], V. Tikhomirov[37,a], Yu.A. Tikhonov[37], S. Timoshenko[37], E.X.L. Ting[1], P. Tipton[170], S. Tisserant[101], S.H. Tlou[33g], A. Tnourji[40], K. Todome[23b,23a], S. Todorova-Nova[132], S. Todt[50], M. Togawa[82], J. Tojo[88], S. Tokár[28a], K. Tokushuku[82], R. Tombs[32], M. Tomoto[82,110], L. Tompkins[142], K.W. Topolnicki[84b], P. Tornambe[102], E. Torrence[122], H. Torres[50], E. Torró Pastor[161], M. Toscani[30], C. Tosciri[39], D.R. Tovey[138], A. Traeet[16], I.S. Trandafir[27b], T. Trefzger[164], A. Tricoli[29], I.M. Trigger[155a], S. Trincaz-Duvoid[126], D.A. Trischuk[26], B. Trocmé[60], A. Trofymov[66], C. Troncon[70a], L. Truong[33c], M. Trzebinski[85], A. Trzupek[85], F. Tsai[144], M. Tsai[105], A. Tsiamis[151],

JHEP06(2023)082

P.V. Tsiareshka[37], S. Tsigaridas[155a], A. Tsirigotis[151,s], V. Tsiskaridze[144], E.G. Tskhadadze[148a], M. Tsopoulou[151], Y. Tsujikawa[86], I.I. Tsukerman[37], V. Tsulaia[17a], S. Tsuno[82], O. Tsur[149], D. Tsybychev[144], Y. Tu[64b], A. Tudorache[27b], V. Tudorache[27b], A.N. Tuna[36], S. Turchikhin[38], I. Turk Cakir[3a], R. Turra[70a], T. Turtuvshin[38], P.M. Tuts[41], S. Tzamarias[151], P. Tzanis[10], E. Tzovara[99], K. Uchida[152], F. Ukegawa[156], P.A. Ulloa Poblete[136c], G. Unal[36], M. Unal[11], A. Undrus[29], G. Unel[158], J. Urban[28b], P. Urquijo[104], G. Usai[8], R. Ushioda[153], M. Usman[107], Z. Uysal[21b], V. Vacek[131], B. Vachon[103], K.O.H. Vadla[124], T. Vafeiadis[36], C. Valderanis[108], E. Valdes Santurio[47a,47b], M. Valente[155a], S. Valentinetti[23b,23a], A. Valero[161], A. Vallier[101], J.A. Valls Ferrer[161], T.R. Van Daalen[137], P. Van Gemmeren[6], M. Van Rijnbach[124,36], S. Van Stroud[95], I. Van Vulpen[113], M. Vanadia[75a,75b], W. Vandelli[36], M. Vandenbroucke[134], E.R. Vandewall[120], D. Vannicola[150], L. Vannoli[57b,57a], R. Vari[74a], E.W. Varnes[7], C. Varni[17a], T. Varol[147], D. Varouchas[66], L. Varriale[161], K.E. Varvell[146], M.E. Vasile[27b], L. Vaslin[40], G.A. Vasquez[163], F. Vazeille[40], T. Vazquez Schroeder[36], J. Veatch[31], V. Vecchio[100], M.J. Veen[102], I. Veliscek[125], L.M. Veloce[154], F. Veloso[129a,129c], S. Veneziano[74a], A. Ventura[69a,69b], A. Verbytskyi[109], M. Verducci[73a,73b], C. Vergis[24], M. Verissimo De Araujo[81b], W. Verkerke[113], J.C. Vermeulen[113], C. Vernieri[142], P.J. Verschuuren[94], M. Vessella[102], M.C. Vetterli[141,aa], A. Vgenopoulos[151], N. Viaux Maira[136f], T. Vickey[138], O.E. Vickey Boeriu[138], G.H.A. Viehhauser[125], L. Vigani[63b], M. Villa[23b,23a], M. Villaplana Perez[161], E.M. Villhauer[52], E. Vilucchi[53], M.G. Vincter[34], G.S. Virdee[20], A. Vishwakarma[52], C. Vittori[23b,23a], I. Vivarelli[145], V. Vladimirov[165], E. Voevodina[109], F. Vogel[108], P. Vokac[131], J. Von Ahnen[48], E. Von Toerne[24], B. Vormwald[36], V. Vorobel[132], K. Vorobev[37], M. Vos[161], J.H. Vossebeld[91], M. Vozak[113], L. Vozdecky[93], N. Vranjes[15], M. Vranjes Milosavljevic[15], M. Vreeswijk[113], R. Vuillermet[36], O. Vujinovic[99], I. Vukotic[39], S. Wada[156], C. Wagner[102], W. Wagner[169], S. Wahdan[169], H. Wahlberg[89], R. Wakasa[156], M. Wakida[110], V.M. Walbrecht[109], J. Walder[133], R. Walker[108], W. Walkowiak[140], A.M. Wang[61], A.Z. Wang[168], C. Wang[62a], C. Wang[62c], H. Wang[17a], J. Wang[64a], P. Wang[44], R.-J. Wang[99], R. Wang[61], R. Wang[6], S.M. Wang[147], S. Wang[62b], T. Wang[62a], W.T. Wang[79], W.X. Wang[62a], X. Wang[14c], X. Wang[160], X. Wang[62c], Y. Wang[62d], Y. Wang[14c], Z. Wang[105], Z. Wang[62d,51,62c], Z. Wang[105], A. Warburton[103], R.J. Ward[20], N. Warrack[59], A.T. Watson[20], M.F. Watson[20], G. Watts[137], B.M. Waugh[95], A.F. Webb[11], C. Weber[29], M.S. Weber[19], S.M. Weber[63a], C. Wei[62a], Y. Wei[125], A.R. Weidberg[125], J. Weingarten[49], M. Weirich[99], C. Weiser[54], C.J. Wells[48], T. Wenaus[29], B. Wendland[49], T. Wengler[36], N.S. Wenke[109], N. Wermes[24], M. Wessels[63a], K. Whalen[122], A.M. Wharton[90], A.S. White[61], A. White[8], M.J. White[1], D. Whiteson[158], L. Wickremasinghe[123], W. Wiedenmann[168], C. Wiel[50], M. Wielers[133], N. Wieseotte[99], C. Wiglesworth[42], L.A.M. Wiik-Fuchs[54], D.J. Wilbern[119], H.G. Wilkens[36], D.M. Williams[41], H.H. Williams[127], S. Williams[32], S. Willocq[102], P.J. Windischhofer[125], F. Winklmeier[122], B.T. Winter[54], M. Wittgen[142], M. Wobisch[96], R. Wölker[125], J. Wollrath[158], M.W. Wolter[85], H. Wolters[129a,129c], V.W.S. Wong[162], A.F. Wongel[48], S.D. Worm[48], B.K. Wosiek[85], K.W. Woźniak[85],

JHEP06(2023)082

K. Wraight[59], J. Wu[14a,14d], M. Wu[64a], M. Wu[112], S.L. Wu[168], X. Wu[56], Y. Wu[62a], Z. Wu[134,62a], J. Wuerzinger[125], T.R. Wyatt[100], B.M. Wynne[52], S. Xella[42], L. Xia[14c], M. Xia[14b], J. Xiang[64c], X. Xiao[105], M. Xie[62a], X. Xie[62a], J. Xiong[17a], I. Xiotidis[145], D. Xu[14a], H. Xu[62a], H. Xu[62a], L. Xu[62a], R. Xu[127], T. Xu[105], W. Xu[105], Y. Xu[14b], Z. Xu[62b], Z. Xu[142], B. Yabsley[146], S. Yacoob[33a], N. Yamaguchi[88], Y. Yamaguchi[153], H. Yamauchi[156], T. Yamazaki[17a], Y. Yamazaki[83], J. Yan[62c], S. Yan[125], Z. Yan[25], H.J. Yang[62c,62d], H.T. Yang[17a], S. Yang[62a], T. Yang[64c], X. Yang[62a], X. Yang[14a], Y. Yang[44], Z. Yang[62a,105], W-M. Yao[17a], Y.C. Yap[48], H. Ye[14c], J. Ye[44], S. Ye[29], X. Ye[62a], Y. Yeh[95], I. Yeletskikh[38], M.R. Yexley[90], P. Yin[41], K. Yorita[166], C.J.S. Young[54], C. Young[142], M. Yuan[105], R. Yuan[62b,j], L. Yue[95], X. Yue[63a], M. Zaazoua[35e], B. Zabinski[85], E. Zaid[52], T. Zakareishvili[148b], N. Zakharchuk[34], S. Zambito[56], J.A. Zamora Saa[136d], J. Zang[152], D. Zanzi[54], O. Zaplatilek[131], S.V. Zeißner[49], C. Zeitnitz[169], J.C. Zeng[160], D.T. Zenger Jr[26], O. Zenin[37], T. Ženiš[28a], S. Zenz[93], S. Zerradi[35a], D. Zerwas[66], B. Zhang[14c], D.F. Zhang[138], G. Zhang[14b], J. Zhang[62b], J. Zhang[6], K. Zhang[14a,14d], L. Zhang[14c], P. Zhang[14a,14d], R. Zhang[168], S. Zhang[105], T. Zhang[152], X. Zhang[62c], X. Zhang[62b], Z. Zhang[17a], Z. Zhang[66], H. Zhao[137], P. Zhao[51], T. Zhao[62b], Y. Zhao[135], Z. Zhao[62a], A. Zhemchugov[38], X. Zheng[62a], Z. Zheng[142], D. Zhong[160], B. Zhou[105], C. Zhou[168], H. Zhou[7], N. Zhou[62c], Y. Zhou[7], C.G. Zhu[62b], C. Zhu[14a,14d], H.L. Zhu[62a], H. Zhu[14a], J. Zhu[105], Y. Zhu[62c], Y. Zhu[62a], X. Zhuang[14a], K. Zhukov[37], V. Zhulanov[37], N.I. Zimine[38], J. Zinsser[63b], M. Ziolkowski[140], L. Živković[15], A. Zoccoli[23b,23a], K. Zoch[56], T.G. Zorbas[138], O. Zormpa[46], W. Zou[41], L. Zwalinski[36]

[1] *Department of Physics, University of Adelaide, Adelaide; Australia*
[2] *Department of Physics, University of Alberta, Edmonton AB; Canada*
[3] [(a)] *Department of Physics, Ankara University, Ankara;* [(b)] *Division of Physics, TOBB University of Economics and Technology, Ankara; Türkiye*
[4] *LAPP, Univ. Savoie Mont Blanc, CNRS/IN2P3, Annecy; France*
[5] *APC, Université Paris Cité, CNRS/IN2P3, Paris; France*
[6] *High Energy Physics Division, Argonne National Laboratory, Argonne IL; United States of America*
[7] *Department of Physics, University of Arizona, Tucson AZ; United States of America*
[8] *Department of Physics, University of Texas at Arlington, Arlington TX; United States of America*
[9] *Physics Department, National and Kapodistrian University of Athens, Athens; Greece*
[10] *Physics Department, National Technical University of Athens, Zografou; Greece*
[11] *Department of Physics, University of Texas at Austin, Austin TX; United States of America*
[12] *Institute of Physics, Azerbaijan Academy of Sciences, Baku; Azerbaijan*
[13] *Institut de Física d'Altes Energies (IFAE), Barcelona Institute of Science and Technology, Barcelona; Spain*
[14] [(a)] *Institute of High Energy Physics, Chinese Academy of Sciences, Beijing;* [(b)] *Physics Department, Tsinghua University, Beijing;* [(c)] *Department of Physics, Nanjing University, Nanjing;* [(d)] *University of Chinese Academy of Science (UCAS), Beijing; China*
[15] *Institute of Physics, University of Belgrade, Belgrade; Serbia*
[16] *Department for Physics and Technology, University of Bergen, Bergen; Norway*
[17] [(a)] *Physics Division, Lawrence Berkeley National Laboratory, Berkeley CA;* [(b)] *University of California, Berkeley CA; United States of America*
[18] *Institut für Physik, Humboldt Universität zu Berlin, Berlin; Germany*
[19] *Albert Einstein Center for Fundamental Physics and Laboratory for High Energy Physics, University of Bern, Bern; Switzerland*

JHEP06(2023)082

[20] School of Physics and Astronomy, University of Birmingham, Birmingham; United Kingdom
[21] [(a)] Department of Physics, Bogazici University, Istanbul; [(b)] Department of Physics Engineering, Gaziantep University, Gaziantep; [(c)] Department of Physics, Istanbul University, Istanbul; [(d)] Istinye University, Sariyer, Istanbul; Türkiye
[22] [(a)] Facultad de Ciencias y Centro de Investigaciónes, Universidad Antonio Nariño, Bogotá; [(b)] Departamento de Física, Universidad Nacional de Colombia, Bogotá; Colombia
[23] [(a)] Dipartimento di Fisica e Astronomia A. Righi, Università di Bologna, Bologna; [(b)] INFN Sezione di Bologna; Italy
[24] Physikalisches Institut, Universität Bonn, Bonn; Germany
[25] Department of Physics, Boston University, Boston MA; United States of America
[26] Department of Physics, Brandeis University, Waltham MA; United States of America
[27] [(a)] Transilvania University of Brasov, Brasov; [(b)] Horia Hulubei National Institute of Physics and Nuclear Engineering, Bucharest; [(c)] Department of Physics, Alexandru Ioan Cuza University of Iasi, Iasi; [(d)] National Institute for Research and Development of Isotopic and Molecular Technologies, Physics Department, Cluj-Napoca; [(e)] University Politehnica Bucharest, Bucharest; [(f)] West University in Timisoara, Timisoara; [(g)] Faculty of Physics, University of Bucharest, Bucharest; Romania
[28] [(a)] Faculty of Mathematics, Physics and Informatics, Comenius University, Bratislava; [(b)] Department of Subnuclear Physics, Institute of Experimental Physics of the Slovak Academy of Sciences, Kosice; Slovak Republic
[29] Physics Department, Brookhaven National Laboratory, Upton NY; United States of America
[30] Universidad de Buenos Aires, Facultad de Ciencias Exactas y Naturales, Departamento de Física, y CONICET, Instituto de Física de Buenos Aires (IFIBA), Buenos Aires; Argentina
[31] California State University, CA; United States of America
[32] Cavendish Laboratory, University of Cambridge, Cambridge; United Kingdom
[33] [(a)] Department of Physics, University of Cape Town, Cape Town; [(b)] iThemba Labs, Western Cape; [(c)] Department of Mechanical Engineering Science, University of Johannesburg, Johannesburg; [(d)] National Institute of Physics, University of the Philippines Diliman (Philippines); [(e)] University of South Africa, Department of Physics, Pretoria; [(f)] University of Zululand, KwaDlangezwa; [(g)] School of Physics, University of the Witwatersrand, Johannesburg; South Africa
[34] Department of Physics, Carleton University, Ottawa ON; Canada
[35] [(a)] Faculté des Sciences Ain Chock, Réseau Universitaire de Physique des Hautes Energies — Université Hassan II, Casablanca; [(b)] Faculté des Sciences, Université Ibn-Tofail, Kénitra; [(c)] Faculté des Sciences Semlalia, Université Cadi Ayyad, LPHEA-Marrakech; [(d)] LPMR, Faculté des Sciences, Université Mohamed Premier, Oujda; [(e)] Faculté des sciences, Université Mohammed V, Rabat; [(f)] Institute of Applied Physics, Mohammed VI Polytechnic University, Ben Guerir; Morocco
[36] CERN, Geneva; Switzerland
[37] Affiliated with an institute covered by a cooperation agreement with CERN
[38] Affiliated with an international laboratory covered by a cooperation agreement with CERN
[39] Enrico Fermi Institute, University of Chicago, Chicago IL; United States of America
[40] LPC, Université Clermont Auvergne, CNRS/IN2P3, Clermont-Ferrand; France
[41] Nevis Laboratory, Columbia University, Irvington NY; United States of America
[42] Niels Bohr Institute, University of Copenhagen, Copenhagen; Denmark
[43] [(a)] Dipartimento di Fisica, Università della Calabria, Rende; [(b)] INFN Gruppo Collegato di Cosenza, Laboratori Nazionali di Frascati; Italy
[44] Physics Department, Southern Methodist University, Dallas TX; United States of America
[45] Physics Department, University of Texas at Dallas, Richardson TX; United States of America
[46] National Centre for Scientific Research "Demokritos", Agia Paraskevi; Greece
[47] [(a)] Department of Physics, Stockholm University; [(b)] Oskar Klein Centre, Stockholm; Sweden
[48] Deutsches Elektronen-Synchrotron DESY, Hamburg and Zeuthen; Germany
[49] Fakultät Physik , Technische Universität Dortmund, Dortmund; Germany
[50] Institut für Kern- und Teilchenphysik, Technische Universität Dresden, Dresden; Germany
[51] Department of Physics, Duke University, Durham NC; United States of America

JHEP06(2023)082

[52] SUPA — School of Physics and Astronomy, University of Edinburgh, Edinburgh; United Kingdom
[53] INFN e Laboratori Nazionali di Frascati, Frascati; Italy
[54] Physikalisches Institut, Albert-Ludwigs-Universität Freiburg, Freiburg; Germany
[55] II. Physikalisches Institut, Georg-August-Universität Göttingen, Göttingen; Germany
[56] Département de Physique Nucléaire et Corpusculaire, Université de Genève, Genève; Switzerland
[57] [(a)] Dipartimento di Fisica, Università di Genova, Genova; [(b)] INFN Sezione di Genova; Italy
[58] II. Physikalisches Institut, Justus-Liebig-Universität Giessen, Giessen; Germany
[59] SUPA — School of Physics and Astronomy, University of Glasgow, Glasgow; United Kingdom
[60] LPSC, Université Grenoble Alpes, CNRS/IN2P3, Grenoble INP, Grenoble; France
[61] Laboratory for Particle Physics and Cosmology, Harvard University, Cambridge MA; United States of America
[62] [(a)] Department of Modern Physics and State Key Laboratory of Particle Detection and Electronics, University of Science and Technology of China, Hefei; [(b)] Institute of Frontier and Interdisciplinary Science and Key Laboratory of Particle Physics and Particle Irradiation (MOE), Shandong University, Qingdao; [(c)] School of Physics and Astronomy, Shanghai Jiao Tong University, Key Laboratory for Particle Astrophysics and Cosmology (MOE), SKLPPC, Shanghai; [(d)] Tsung-Dao Lee Institute, Shanghai; China
[63] [(a)] Kirchhoff-Institut für Physik, Ruprecht-Karls-Universität Heidelberg, Heidelberg; [(b)] Physikalisches Institut, Ruprecht-Karls-Universität Heidelberg, Heidelberg; Germany
[64] [(a)] Department of Physics, Chinese University of Hong Kong, Shatin, N.T., Hong Kong; [(b)] Department of Physics, University of Hong Kong, Hong Kong; [(c)] Department of Physics and Institute for Advanced Study, Hong Kong University of Science and Technology, Clear Water Bay, Kowloon, Hong Kong; China
[65] Department of Physics, National Tsing Hua University, Hsinchu; Taiwan
[66] IJCLab, Université Paris-Saclay, CNRS/IN2P3, 91405, Orsay; France
[67] Department of Physics, Indiana University, Bloomington IN; United States of America
[68] [(a)] INFN Gruppo Collegato di Udine, Sezione di Trieste, Udine; [(b)] ICTP, Trieste; [(c)] Dipartimento Politecnico di Ingegneria e Architettura, Università di Udine, Udine; Italy
[69] [(a)] INFN Sezione di Lecce; [(b)] Dipartimento di Matematica e Fisica, Università del Salento, Lecce; Italy
[70] [(a)] INFN Sezione di Milano; [(b)] Dipartimento di Fisica, Università di Milano, Milano; Italy
[71] [(a)] INFN Sezione di Napoli; [(b)] Dipartimento di Fisica, Università di Napoli, Napoli; Italy
[72] [(a)] INFN Sezione di Pavia; [(b)] Dipartimento di Fisica, Università di Pavia, Pavia; Italy
[73] [(a)] INFN Sezione di Pisa; [(b)] Dipartimento di Fisica E. Fermi, Università di Pisa, Pisa; Italy
[74] [(a)] INFN Sezione di Roma; [(b)] Dipartimento di Fisica, Sapienza Università di Roma, Roma; Italy
[75] [(a)] INFN Sezione di Roma Tor Vergata; [(b)] Dipartimento di Fisica, Università di Roma Tor Vergata, Roma; Italy
[76] [(a)] INFN Sezione di Roma Tre; [(b)] Dipartimento di Matematica e Fisica, Università Roma Tre, Roma; Italy
[77] [(a)] INFN-TIFPA; [(b)] Università degli Studi di Trento, Trento; Italy
[78] Universität Innsbruck, Department of Astro and Particle Physics, Innsbruck; Austria
[79] University of Iowa, Iowa City IA; United States of America
[80] Department of Physics and Astronomy, Iowa State University, Ames IA; United States of America
[81] [(a)] Departamento de Engenharia Elétrica, Universidade Federal de Juiz de Fora (UFJF), Juiz de Fora; [(b)] Universidade Federal do Rio De Janeiro COPPE/EE/IF, Rio de Janeiro; [(c)] Instituto de Física, Universidade de São Paulo, São Paulo; [(d)] Rio de Janeiro State University, Rio de Janeiro; Brazil
[82] KEK, High Energy Accelerator Research Organization, Tsukuba; Japan
[83] Graduate School of Science, Kobe University, Kobe; Japan
[84] [(a)] AGH University of Science and Technology, Faculty of Physics and Applied Computer Science, Krakow; [(b)] Marian Smoluchowski Institute of Physics, Jagiellonian University, Krakow; Poland
[85] Institute of Nuclear Physics Polish Academy of Sciences, Krakow; Poland
[86] Faculty of Science, Kyoto University, Kyoto; Japan
[87] Kyoto University of Education, Kyoto; Japan

JHEP06(2023)082

[88] Research Center for Advanced Particle Physics and Department of Physics, Kyushu University, Fukuoka ; Japan
[89] Instituto de Física La Plata, Universidad Nacional de La Plata and CONICET, La Plata; Argentina
[90] Physics Department, Lancaster University, Lancaster; United Kingdom
[91] Oliver Lodge Laboratory, University of Liverpool, Liverpool; United Kingdom
[92] Department of Experimental Particle Physics, Jožef Stefan Institute and Department of Physics, University of Ljubljana, Ljubljana; Slovenia
[93] School of Physics and Astronomy, Queen Mary University of London, London; United Kingdom
[94] Department of Physics, Royal Holloway University of London, Egham; United Kingdom
[95] Department of Physics and Astronomy, University College London, London; United Kingdom
[96] Louisiana Tech University, Ruston LA; United States of America
[97] Fysiska institutionen, Lunds universitet, Lund; Sweden
[98] Departamento de Física Teorica C-15 and CIAFF, Universidad Autónoma de Madrid, Madrid; Spain
[99] Institut für Physik, Universität Mainz, Mainz; Germany
[100] School of Physics and Astronomy, University of Manchester, Manchester; United Kingdom
[101] CPPM, Aix-Marseille Université, CNRS/IN2P3, Marseille; France
[102] Department of Physics, University of Massachusetts, Amherst MA; United States of America
[103] Department of Physics, McGill University, Montreal QC; Canada
[104] School of Physics, University of Melbourne, Victoria; Australia
[105] Department of Physics, University of Michigan, Ann Arbor MI; United States of America
[106] Department of Physics and Astronomy, Michigan State University, East Lansing MI; United States of America
[107] Group of Particle Physics, University of Montreal, Montreal QC; Canada
[108] Fakultät für Physik, Ludwig-Maximilians-Universität München, München; Germany
[109] Max-Planck-Institut für Physik (Werner-Heisenberg-Institut), München; Germany
[110] Graduate School of Science and Kobayashi-Maskawa Institute, Nagoya University, Nagoya; Japan
[111] Department of Physics and Astronomy, University of New Mexico, Albuquerque NM; United States of America
[112] Institute for Mathematics, Astrophysics and Particle Physics, Radboud University/Nikhef, Nijmegen; Netherlands
[113] Nikhef National Institute for Subatomic Physics and University of Amsterdam, Amsterdam; Netherlands
[114] Department of Physics, Northern Illinois University, DeKalb IL; United States of America
[115] [(a)] New York University Abu Dhabi, Abu Dhabi; [(b)] United Arab Emirates University, Al Ain; [(c)] University of Sharjah, Sharjah; United Arab Emirates
[116] Department of Physics, New York University, New York NY; United States of America
[117] Ochanomizu University, Otsuka, Bunkyo-ku, Tokyo; Japan
[118] Ohio State University, Columbus OH; United States of America
[119] Homer L. Dodge Department of Physics and Astronomy, University of Oklahoma, Norman OK; United States of America
[120] Department of Physics, Oklahoma State University, Stillwater OK; United States of America
[121] Palacký University, Joint Laboratory of Optics, Olomouc; Czech Republic
[122] Institute for Fundamental Science, University of Oregon, Eugene, OR; United States of America
[123] Graduate School of Science, Osaka University, Osaka; Japan
[124] Department of Physics, University of Oslo, Oslo; Norway
[125] Department of Physics, Oxford University, Oxford; United Kingdom
[126] LPNHE, Sorbonne Université, Université Paris Cité, CNRS/IN2P3, Paris; France
[127] Department of Physics, University of Pennsylvania, Philadelphia PA; United States of America
[128] Department of Physics and Astronomy, University of Pittsburgh, Pittsburgh PA; United States of America
[129] [(a)] Laboratório de Instrumentação e Física Experimental de Partículas — LIP, Lisboa; [(b)] Departamento de Física, Faculdade de Ciências, Universidade de Lisboa, Lisboa; [(c)] Departamento

JHEP06(2023)082

de Física, Universidade de Coimbra, Coimbra; [(d)] *Centro de Física Nuclear da Universidade de Lisboa, Lisboa;* [(e)] *Departamento de Física, Universidade do Minho, Braga;* [(f)] *Departamento de Física Teórica y del Cosmos, Universidad de Granada, Granada (Spain);* [(g)] *Departamento de Física, Instituto Superior Técnico, Universidade de Lisboa, Lisboa; Portugal*

[130] *Institute of Physics of the Czech Academy of Sciences, Prague; Czech Republic*

[131] *Czech Technical University in Prague, Prague; Czech Republic*

[132] *Charles University, Faculty of Mathematics and Physics, Prague; Czech Republic*

[133] *Particle Physics Department, Rutherford Appleton Laboratory, Didcot; United Kingdom*

[134] *IRFU, CEA, Université Paris-Saclay, Gif-sur-Yvette; France*

[135] *Santa Cruz Institute for Particle Physics, University of California Santa Cruz, Santa Cruz CA; United States of America*

[136] [(a)] *Departamento de Física, Pontificia Universidad Católica de Chile, Santiago;* [(b)] *Millennium Institute for Subatomic physics at high energy frontier (SAPHIR), Santiago;* [(c)] *Instituto de Investigación Multidisciplinario en Ciencia y Tecnología, y Departamento de Física, Universidad de La Serena;* [(d)] *Universidad Andres Bello, Department of Physics, Santiago;* [(e)] *Instituto de Alta Investigación, Universidad de Tarapacá, Arica;* [(f)] *Departamento de Física, Universidad Técnica Federico Santa María, Valparaíso; Chile*

[137] *Department of Physics, University of Washington, Seattle WA; United States of America*

[138] *Department of Physics and Astronomy, University of Sheffield, Sheffield; United Kingdom*

[139] *Department of Physics, Shinshu University, Nagano; Japan*

[140] *Department Physik, Universität Siegen, Siegen; Germany*

[141] *Department of Physics, Simon Fraser University, Burnaby BC; Canada*

[142] *SLAC National Accelerator Laboratory, Stanford CA; United States of America*

[143] *Department of Physics, Royal Institute of Technology, Stockholm; Sweden*

[144] *Departments of Physics and Astronomy, Stony Brook University, Stony Brook NY; United States of America*

[145] *Department of Physics and Astronomy, University of Sussex, Brighton; United Kingdom*

[146] *School of Physics, University of Sydney, Sydney; Australia*

[147] *Institute of Physics, Academia Sinica, Taipei; Taiwan*

[148] [(a)] *E. Andronikashvili Institute of Physics, Iv. Javakhishvili Tbilisi State University, Tbilisi;* [(b)] *High Energy Physics Institute, Tbilisi State University, Tbilisi;* [(c)] *University of Georgia, Tbilisi; Georgia*

[149] *Department of Physics, Technion, Israel Institute of Technology, Haifa; Israel*

[150] *Raymond and Beverly Sackler School of Physics and Astronomy, Tel Aviv University, Tel Aviv; Israel*

[151] *Department of Physics, Aristotle University of Thessaloniki, Thessaloniki; Greece*

[152] *International Center for Elementary Particle Physics and Department of Physics, University of Tokyo, Tokyo; Japan*

[153] *Department of Physics, Tokyo Institute of Technology, Tokyo; Japan*

[154] *Department of Physics, University of Toronto, Toronto ON; Canada*

[155] [(a)] *TRIUMF, Vancouver BC;* [(b)] *Department of Physics and Astronomy, York University, Toronto ON; Canada*

[156] *Division of Physics and Tomonaga Center for the History of the Universe, Faculty of Pure and Applied Sciences, University of Tsukuba, Tsukuba; Japan*

[157] *Department of Physics and Astronomy, Tufts University, Medford MA; United States of America*

[158] *Department of Physics and Astronomy, University of California Irvine, Irvine CA; United States of America*

[159] *Department of Physics and Astronomy, University of Uppsala, Uppsala; Sweden*

[160] *Department of Physics, University of Illinois, Urbana IL; United States of America*

[161] *Instituto de Física Corpuscular (IFIC), Centro Mixto Universidad de Valencia — CSIC, Valencia; Spain*

[162] *Department of Physics, University of British Columbia, Vancouver BC; Canada*

[163] *Department of Physics and Astronomy, University of Victoria, Victoria BC; Canada*

[164] *Fakultät für Physik und Astronomie, Julius-Maximilians-Universität Würzburg, Würzburg; Germany*

JHEP06(2023)082

[165] Department of Physics, University of Warwick, Coventry; United Kingdom
[166] Waseda University, Tokyo; Japan
[167] Department of Particle Physics and Astrophysics, Weizmann Institute of Science, Rehovot; Israel
[168] Department of Physics, University of Wisconsin, Madison WI; United States of America
[169] Fakultät für Mathematik und Naturwissenschaften, Fachgruppe Physik, Bergische Universität Wuppertal, Wuppertal; Germany
[170] Department of Physics, Yale University, New Haven CT; United States of America

[a] Also Affiliated with an institute covered by a cooperation agreement with CERN
[b] Also at Borough of Manhattan Community College, City University of New York, New York NY; United States of America
[c] Also at Bruno Kessler Foundation, Trento; Italy
[d] Also at Center for High Energy Physics, Peking University; China
[e] Also at Centro Studi e Ricerche Enrico Fermi; Italy
[f] Also at CERN, Geneva; Switzerland
[g] Also at Département de Physique Nucléaire et Corpusculaire, Université de Genève, Genève; Switzerland
[h] Also at Departament de Fisica de la Universitat Autonoma de Barcelona, Barcelona; Spain
[i] Also at Department of Financial and Management Engineering, University of the Aegean, Chios; Greece
[j] Also at Department of Physics and Astronomy, Michigan State University, East Lansing MI; United States of America
[k] Also at Department of Physics and Astronomy, University of Louisville, Louisville, KY; United States of America
[l] Also at Department of Physics, Ben Gurion University of the Negev, Beer Sheva; Israel
[m] Also at Department of Physics, California State University, East Bay; United States of America
[n] Also at Department of Physics, California State University, Sacramento; United States of America
[o] Also at Department of Physics, King's College London, London; United Kingdom
[p] Also at Department of Physics, University of Fribourg, Fribourg; Switzerland
[q] Also at Department of Physics, University of Thessaly; Greece
[r] Also at Department of Physics, Westmont College, Santa Barbara; United States of America
[s] Also at Hellenic Open University, Patras; Greece
[t] Also at Institucio Catalana de Recerca i Estudis Avancats, ICREA, Barcelona; Spain
[u] Also at Institut für Experimentalphysik, Universität Hamburg, Hamburg; Germany
[v] Also at Institute of Particle Physics (IPP); Canada
[w] Also at Institute of Physics, Azerbaijan Academy of Sciences, Baku; Azerbaijan
[x] Also at Institute of Theoretical Physics, Ilia State University, Tbilisi; Georgia
[y] Also at Lawrence Livermore National Laboratory, Livermore; United States of America
[z] Also at The Collaborative Innovation Center of Quantum Matter (CICQM), Beijing; China
[aa] Also at TRIUMF, Vancouver BC; Canada
[ab] Also at Università di Napoli Parthenope, Napoli; Italy
[ac] Also at University of Chinese Academy of Sciences (UCAS), Beijing; China
[ad] Also at University of Colorado Boulder, Department of Physics, Colorado; United States of America
[ae] Also at Washington College, Maryland; United States of America
[af] Also at Yeditepe University, Physics Department, Istanbul; Türkiye
[ag] Also at Physics Department, An-Najah National University, Nablus; Palestine
[*] Deceased

JHEP06(2023)082